A multiple proxy and model study of Cretaceous upper ocean temperatures and atmospheric CO_2 concentrations

Karen L. Bice,[1] Daniel Birgel,[2] Philip A. Meyers,[3] Kristina A. Dahl,[1,4] Kai-Uwe Hinrichs,[2] and Richard D. Norris[5]

[1] We estimate tropical Atlantic upper ocean temperatures using oxygen isotope and Mg/Ca ratios in well-preserved planktonic foraminifera extracted from Albian through Santonian black shales recovered during Ocean Drilling Program Leg 207 (North Atlantic Demerara Rise). On the basis of a range of plausible assumptions regarding seawater composition at the time the data support temperatures between 33° and 42°C. In our low-resolution data set spanning ~84–100 Ma a local temperature maximum occurs in the late Turonian, and a possible minimum occurs in the mid to early late Cenomanian. The relation between single species foraminiferal $\delta^{18}O$ and Mg/Ca suggests that the ratio of magnesium to calcium in the Turonian-Coniacian ocean may have been lower than in the Albian-Cenomanian ocean, perhaps coincident with an ocean $^{87}Sr/^{86}Sr$ minimum. The carbon isotopic compositions of distinct marine algal biomarkers were measured in the same sediment samples. The $\delta^{13}C$ values of phytane, combined with foraminiferal $\delta^{13}C$ and inferred temperatures, were used to estimate atmospheric carbon dioxide concentrations through this interval. Estimates of atmospheric CO_2 concentrations range between 600 and 2400 ppmv. Within the uncertainty in the various proxies, there is only a weak overall correspondence between higher (lower) tropical temperatures and more (less) atmospheric CO_2. The GENESIS climate model underpredicts tropical Atlantic temperatures inferred from ODP Leg 207 foraminiferal $\delta^{18}O$ and Mg/Ca when we specify approximate CO_2 concentrations estimated from the biomarker isotopes in the same samples. Possible errors in the temperature and CO_2 estimates and possible deficiencies in the model are discussed. The potential for and effects of substantially higher atmospheric methane during Cretaceous anoxic events, perhaps derived from high fluxes from the oxygen minimum zone, are considered in light of recent work that shows a quadratic relation between increased methane flux and atmospheric CH_4 concentrations. With 50 ppm CH_4, GENESIS sea surface temperatures approximate the minimum upper ocean temperatures inferred from proxy data when CO_2 concentrations specified to the model are near those inferred using the phytane $\delta^{13}C$ proxy. However, atmospheric CO_2 concentrations of 3500 ppm or more are still required in the model in order to reproduce inferred maximum temperatures.

1. Introduction

[2] The concentration of carbon dioxide in the atmosphere is believed to be a primary determinant of climate [*Royer et al.*, 2004]. Model studies indicate that the direct radiative effects and water vapor feedbacks accompanying a change from 500 to 1000 ppm CO_2 (values at the lower end of mid-Cretaceous CO_2 estimates) have a greater effect on Earth's surface temperature than the combined temperature effects of paleogeographic and solar luminosity changes over the past 90 million years [*Bice et al.*, 2000; *Bice and Norris*, 2002]. Estimates of Cretaceous CO_2 concentrations have been made using a variety of terrestrial and marine proxies, including the carbon isotopic composition of specific organic compounds. The resulting estimates for an individual geologic stage can vary widely [*Royer et al.*, 2001; *Bice and Norris*, 2002, and references therein]. In a model-data study, *Bice and Norris* [2002] suggested that in the mid-Cretaceous at least, this variability may be real, which points out the need for a multiple proxy approach in order to more reliably constrain paleo-CO_2 concentrations.

[3] One of the principal objectives of Ocean Drilling Program (ODP) Leg 207 was to recover Cretaceous and Paleogene strata to reconstruct the history of low-latitude sea surface temperatures. Studies of well preserved Cenomanian and Turonian planktonic foraminifera from Deep Sea Drilling Program (DSDP) Site 144 (redrilled as Site

---

[1]Department of Geology and Geophysics, Woods Hole Oceanographic Institution, Woods Hole, Massachusetts, USA.

[2]Research Center Ocean Margins, University of Bremen, Bremen, Germany.

[3]Department of Geological Sciences, University of Michigan, Ann Arbor, Michigan, USA.

[4]Now at Scripps Institution of Oceanography, La Jolla, California, USA.

[5]Scripps Institution of Oceanography, La Jolla, California, USA.

1257 during Leg 207) can be interpreted as evidence for unusually warm surface ocean temperatures, conservatively calculated between 30° and 35°C [*Norris et al.*, 2002; *Wilson et al.*, 2002]. In combination with data from higher paleolatitudes, these results raise the possibility that atmospheric carbon dioxide concentrations were considerably higher in the early Late Cretaceous than have been estimated by many other proxy studies [*Bice and Norris*, 2002; *Bice et al.*, 2003]. However, studies of DSDP Site 144, as well as other tropical Cretaceous sites, have not attempted to determine both upper ocean temperatures and pCO_2 from the same sediment samples. Sediments recovered during Leg 207 include an expanded sequence of Albian-Santonian organic-rich mudstones (black shales) with very well preserved to excellently preserved microfossils and well preserved organic matter. These sites, then, allow the application of a proxy-CO_2 technique based on the isotopic composition of individual organic compounds and paleotemperature estimates from foraminiferal oxygen isotope and Mg/Ca ratios.

[4] We describe a unique study in which multiple climate proxy measurements were made in order to simultaneously estimate tropical upper ocean paleotemperatures and atmospheric CO_2 concentrations during the time of deposition of Cretaceous black shales. Two purported temperature proxies (foraminiferal $\delta^{18}O$ and Mg/Ca) and a purported pCO_2 proxy ($\delta^{13}C$ of marine organic matter) were measured on Leg 207 samples that contain at least 7% total organic carbon. The samples come from ODP Sites 1257, 1258 and 1260. The multiproxy approach decreases the uncertainty inherent in a study in which the value of an environmental variable (for example, temperature, as needed in the CO_2 estimation) must be assumed based on data taken elsewhere or from a possibly different time interval.

[5] Numerical climate model experiments were performed in order to determine whether different tropical temperature and atmospheric CO_2 concentrations inferred from the multiproxy data are mutually consistent and plausible, and which model results are more/less plausible from a global climate perspective. Given the potential for a higher methane flux to the atmosphere during the mid-Cretaceous and the quadratic relation between increased methane flux and atmospheric CH_4 concentrations [*Pavlov et al.*, 2003], we also use the climate model to examine the potential effect of greater atmospheric methane on upper ocean temperatures during Cretaceous anoxic events.

2. Methods

[6] ODP Leg 207 drilled five sites in a depth transect on Demerara Rise, off Suriname, South America [*Erbacher et al.*, 2004]. This study uses sediments from Sites 1257 (latitude 9.45°N, water depth 2951 m), 1258 (latitude 9.43°N, water depth 3192 m) and 1260 (latitude 9.27°N, water depth 2548 m). These are poorly consolidated laminated, calcareous organic-rich claystones (black shales) of late Albian through Santonian age. The samples come from whole round cores cut on the *JOIDES Resolution* catwalk and frozen shipboard at −80°C. Calcium carbonate content ranges from 25 to 65 weight %, and total organic carbon ranges from 7 to 22 weight %. Absolute ages of our samples

were estimated through a combination of shipboard biostratigraphy and shore-based magnetostratigraphy [*Erbacher et al.*, 2004]. The uncertainty in absolute ages varies, but is estimated as less than 1 million years.

2.1. Paleotemperatures From Stable Isotopes

[7] For stable isotope and Mg/Ca analyses, the frozen sediments were freeze dried and partly crushed using a porcelain mortar and pestle. Following a test of various cleaning procedures [*Bice and Norris*, 2005], the sediments were soaked in undiluted Clorox bleach for 2 hours, washed, and dried, then soaked for 1 hour in undiluted bleach, washed and dried. Well-preserved foraminifera were picked and, if necessary, were sonicated briefly to remove remaining adhering material.

[8] Single species stable isotope analyses were made of 2 to 25 individual whole planktonic foraminifera, primarily *Hedbergella delrioensis*, *Heterohelix globulosa* and *Whiteinella baltica*, from samples reported by *Bice and Norris* [2005] as having good, very good, or excellent preservation. Oxygen and carbon isotope ratios were measured on a Finnigan MAT 252 mass spectrometer with an automated Kiel carbonate device at Woods Hole Oceanographic Institution. Instrument precision is ±0.07 for $\delta^{18}O$ and ±0.03 for $\delta^{13}C$. Results are reported relative to the Vienna Pee Dee Belemnite (PDB) isotope standard and are given in Table 1.

[9] Upper ocean paleotemperatures are estimated from foraminiferal $\delta^{18}O$ using the equation of *Erez and Luz* [1983]. Ambient water $\delta^{18}O$ value (δ_w) is estimated (relative to Standard Mean Ocean Water, SMOW) and is converted to the PDB scale by subtracting 0.27‰ [*Hut*, 1987]. We estimate local δ_w assuming an "ice-free" Cretaceous mean ocean δ_w of −1.25‰ SMOW [*Shackleton and Kennett*, 1975; *Wallmann*, 2001] and adjusting for average latitudinal variations in evaporation and precipitation controls on $\delta^{18}O$ by analogy with modern oceans [*Zachos et al.*, 1994] between 4° and 19° latitude. This is the range of paleolatitudes (including estimated error) for Demerara Rise based on linear interpolation between two paleolatitudes calculated by *Suganuma and Ogg* [2006]: 14.8°N (±5.2°) at ∼102 Ma and 3.6°N (±2.7°) at ∼70 Ma (Table 2). The resulting range of δ_w values used to calculate paleotemperatures is −0.40‰ to −0.54‰ SMOW.

2.2. Mg/Ca From ICP-MS and SIMS

[10] Mg/Ca ratios were measured with a high-resolution sector field inductively coupled plasma mass spectrometer (ICP-MS, Finnegan Element2) at Woods Hole Oceanographic Institution. Initial sample weights were ∼200 μg, consisting of 30–80 individual Cretaceous planktonics picked from the 150–250 μm sieve fraction of the washed sediments prepared for stable isotope analyses. Samples for ICP-MS were weighed and crushed gently between two glass slides in order to open the individual foraminifer chambers for effective cleaning. Samples were then subjected to a series of cleaning treatments designed to remove clays, metal oxides, and organic matter from the tests [*Boyle and Keigwin*, 1985; *Rosenthal et al.*, 1995; *Boyle and Rosenthal*, 1996]. Cleaned carbonate was dissolved in 2% nitric acid. Note that prior to the Mg/Ca cleaning procedure,

Table 1. Average Stable Isotope and Mg/Ca Values for Single Species Cretaceous Samples

Sample	Depth, mbsf	Age	Species	Size Fraction, μm	Average $\delta^{13}C$, ‰ PDB	Average $\delta^{18}O$, ‰ PDB	Mg/Ca, mmol/mol
207-1257C-11R-1, 84–89 cm	178.84	Santonian	*Hedbergella delrioensis*	150–250	1.45	−4.17	
207-1257C-11R-1, 84–89 cm	178.84	Santonian	*Heterohelix globulosa*	212–250	1.17	−4.08	
207-1257C-11R-1, 84–89 cm	178.84	Santonian	*Marginotruncana sinuosa*	>250	1.71	−4.05	
207-1257C-13R-2, 120–140 cm	200.00	Coniacian	*Hedbergella delrioensis*	150–250	1.54	−4.10	
207-1257C-13R-2, 120–140 cm	200.00	Coniacian	*Heterohelix globulosa*	212–250	1.64	−4.20	5.73
207-1257C-13R-2, 120–140 cm	200.00	Coniacian	*Whiteinella baltica*	>250	1.35	−4.31	4.45
207-1257C-14R-1, 76–82 cm	207.76	Turonian	*Hedbergella delrioensis*	150–250	1.45	−4.22	
207-1257C-14R-1, 76–82 cm	207.76	Turonian	*Heterohelix globulosa*	212–250	1.84	−4.28	4.97
207-1257C-14R-1, 76–82 cm	207.76	Turonian	*Whiteinella baltica*	>250	1.25	−4.42	3.96
14-144-4R-3, 72–75 cm	216.72	Cenomanian	*Hedbergella delrioensis*	125–150	1.31	−4.04	5.44
14-144-4R-3, 72–75 cm	216.72	Cenomanian	*Heterohelix moremani*	125–150	0.13	−4.06	7.90
14-144-4R-3, 72–75 cm	216.72	Cenomanian	*Globigerinelloides*	125–150	0.54	−3.76	6.26
207-1258B-51R-2, 10–20 cm	427.85	Cenomanian	*Whiteinella baltica*	>150	0.88	−3.93	4.59
207-1258B-54R-3, 10–30 cm	444.48	Cenomanian	*Hedbergella delrioensis*	150–250	0.40	−3.92	6.32
207-1258B-55R-3, 68–88 cm	448.37	l. Albian	*Hedbergella delrioensis*	150–250	1.85	−3.90	5.85
207-1258B-55R-3, 68–88 cm	448.37	l. Albian	*Ticinella primula*	150–250	1.70	−4.12	
207-1260B-34R-2, 10–17 cm	407.30	Turonian	*Hedbergella delrioensis*	>250	1.32	−4.82	4.45
207-1260B-34R-2, 10–17 cm	407.30	Turonian	*Heterohelix globulosa*	150–250	1.32	−4.73	
207-1260B-37R-1, 10–16 cm	434.60	Cenomanian	*Hedbergella delrioensis*	150–250	1.08	−3.37	5.24
207-1260B-34R-2, 10–17 cm	434.60	Cenomanian	*Globigerinelloides*	150–250	1.00	−3.50	
207-1260B-38R-1, 84–86 cm	444.94	Cenomanian	*Hedbergella delrioensis*	150–250	2.08	−3.74	
207-1260B-39R-1, 115–122 cm	454.85	Cenomanian	*Hedbergella delrioensis*	150–250	1.28	−4.31	5.98
207-1260B-41R-1, 114–120 cm	473.84	Cenomanian	*Hedbergella delrioensis*	150–250	1.00	−4.31	5.61

the black shale samples had been washed using an undiluted bleach procedure, which has been shown to be an efficient way to remove remnant organic matter [*Bice and Norris*, 2005] that might otherwise bias results toward high Mg/Ca values [*Martin and Lea*, 2002]. Mg and Ca concentrations were determined in low-resolution mode by averaging measurements from 74 scans. Ions were counted in analog mode. A standard containing high-purity elements in ratios consistent with those observed in foraminifera and a blank of 2% nitric acid were run between every four samples.

Instrumental precision for Mg/Ca, based on repeated measurements of a series of standards, is 0.03 mmol/mol.

[11] In Cenomanian sample 207-1260B-37R-1, 10–16 cm, the primary calcite Mg/Ca ratio of *H. delrioensis* was determined using secondary ion mass spectrometry (SIMS) [*Bice et al.*, 2005]. In ~10% of *H. delrioensis* individuals in this sample, the outermost 1 or 2 chambers are filled with spar calcite. The foraminifer shells otherwise appear to be very well preserved. It was possible to pick enough spar-free individuals for two stable isotope analyses, but because

Table 2. Sample Age, Paleolatitude, and Temperatures Inferred From Foraminiferal $\delta^{18}O$ and Mg/Ca[a]

Sample	Estimated Age, Ma	Paleolatitude	Species	T From $\delta^{18}O$ (No pH Adjustment), °C	T from Mg/Ca Ocean Mg/Ca = 1.0	Ocean Mg/Ca = 1.5
207-1257C-11R-1, 84–89 cm	84	9° (±4°)	*H. delrioensis*	34.1		
207-1257C-11R-1, 84–89 cm	84	9° (±4°)	*H. globulosa*	33.7		
207-1257C-11R-1, 84–89 cm	84	9° (±4°)	*M. sinuosa*	33.5		
207-1257C-13R-2, 120–140 cm	88	10° (±4°)	*H. delrioensis*	33.8		
207-1257C-13R-2, 120–140 cm	88	10° (±4°)	*H. globulosa*	34.2	40.5	
207-1257C-13R-2, 120–140 cm	88	10° (±4°)	*W. baltica*	34.8	38.0	
207-1257C-14R-1, 76–82 cm	89.5	10° (±4°)	*H. delrioensis*	34.4		
207-1257C-14R-1, 76–82 cm	89.5	10° (±4°)	*H. globulosa*	34.6	39.1	
207-1257C-14R-1, 76–82 cm	89.5	10° (±4°)	*W. baltica*	35.3	36.8	
14-144-4R-3, 72–75 cm	93.5	12° (±5°)	*H. delrioensis*	33.5	40.0	35.9
14-144-4R-3, 72–75 cm	93.5	12° (±5°)	*H. moremani*	33.6	43.7	39.6
14-144-4R-3, 72–75 cm	93.5	12° (±5°)	*Globigerinelloides*	32.2	41.4	37.3
207-1258B-51R-2, 10–20 cm	96	13° (±5°)	*W. baltica*	33.0	38.3	34.2
207-1258B-54R-3, 10–30 cm	98	13° (±5°)	*H. delrioensis*	32.9	41.5	37.4
207-1258B-55R-3, 68–88 cm	99	14° (±5°)	*H. delrioensis*	32.8	40.7	36.6
207-1258B-55R-3, 68–88 cm	99	14° (±5°)	*Ticinella primula*	33.9		
207-1260B-34R-2, 10–17 cm	91	11° (±5°)	*H. delrioensis*	37.2	38.0	
207-1260B-34R-2, 10–17 cm	91	11° (±5°)	*H. globulosa*	36.7		
207-1260B-37R-1, 10–16 cm	95	12° (±5°)	*H. delrioensis*	30.3	39.6	35.5
207-1260B-37R-1, 10–16 cm	95	12° (±5°)	*Globigerinelloides*	30.9		
207-1260B-38R-1, 84–86 cm	96	13° (±5°)	*H. delrioensis*	32.1		
207-1260B-39R-1, 115–122 cm	97	13° (±5°)	*H. delrioensis*	34.8	40.9	36.9
207-1260B-41R-1, 114–120 cm	98.5	14° (±5°)	*H. delrioensis*	34.8	40.3	36.2

[a]Absolute ages of samples given in Table 1 are estimated from sedimentation rate curves for the Leg 207 sites [*Erbacher et al.*, 2004] and have an estimated uncertainty of ±1 million years.

of the high mass of material required for one ICP-MS analysis and the rarity and low mass of planktonics in the black shales, ICP-MS could not be used to generate a reliable Mg/Ca ratio for this sample. With SIMS, less than 1 ng of material is removed in individual spots of <10 μm diameter, with an instrumental precision for Mg/Ca of better than 1%. The high-resolution capability of SIMS allowed us to target pristine calcite in the tests while avoiding contaminant diagenetic calcite. The full SIMS technique used to examine this sample and other Demerara Rise planktonics is described by *Bice et al.* [2005].

[12] For comparison, we also include here Mg/Ca values for three species in one Cenomanian sample from DSDP Site 144 (Table 1), which were also generated at WHOI using the ICP-MS technique described above. The stable isotope values for these species are from *Norris et al.* [2002]. Because no unwashed sediment remained, these samples were not analyzed for bulk carbonate, bulk organic or biomarker isotope ratios.

[13] Considerable uncertainty surrounds the use of Mg/Ca ratios as a paleotemperature proxy. Calibrations of the Mg/Ca proxy have been made for various modern species [*Nürnberg et al.*, 1996; *Rosenthal et al.*, 1997; *Lea et al.*, 1999; *Elderfield and Ganssen*, 2000] and these exhibit considerable variance, but the use of this technique for Cretaceous reconstructions is even more problematic. First, it is not known what exact correspondence, if any, there is between ambient water temperature and the Mg/Ca of test carbonate in extinct planktonic foraminifera. There is also uncertainty in the reconstruction of ancient ocean Mg/Ca, which is believed to have changed considerably though time [*Stanley and Hardie*, 1998]. Parallel problems exist with the oxygen stable isotope paleotemperature proxy: we can never be sure what the actual fractionation relation is for an extinct species and we must make plausible assumptions about the isotopic composition of ancient ambient seawater.

[14] As an experiment here, we first assume the overall temperature-Mg/Ca relation observed in many modern foraminifer species (increasing calcite Mg/Ca ratio with increasing temperature) and examine the relation between the raw foraminiferal $\delta^{18}O$ and Mg/Ca for single species samples. Second, we assume the specific Mg/Ca paleotemperature equation given by *Elderfield and Ganssen* [2000] for the modern species *Globigerinoides sacculifer*. In all core top species considered by Elderfield and Ganssen, *G. sacculifer* has the highest calcification temperature and may therefore be the best available analog for warm paleoclimate reconstructions. The molar ratio of Mg to Ca in the Cretaceous ocean is first assumed to be 1 [*Stanley and Hardie*, 1998] and the modern ocean ratio is taken as 5. We further assume that the temperature:Mg/Ca relation scales linearly with ocean Mg/Ca, though there is recent experimental evidence to suggest this may not be true [*Ries*, 2004]. Foraminiferal Mg/Ca values and the resulting paleotemperature estimates are given in Tables 1 and 2.

2.3. CO$_2$ Estimates From Biomarker $\delta^{13}C$

[15] For lipid biomarker analyses, frozen sediments were freeze dried and homogenized. Extraction and measurement procedures were performed at the Research Center Ocean Margins at the University of Bremen. Biomarker lipids were extracted by repeated ultrasonication with dichloromethane/methanol (3:1 v/v). The apolar fraction (hydrocarbons) was separated from the total extract using Supelco LC-NH2 glass cartridges (500 mg sorbent) with 4 ml of *n*-hexane as eluent. Elemental sulfur was removed from the hydrocarbon fraction by adding acid-activated copper. Individual compounds were identified by coupled gas chromatography–mass spectrometry using a Thermo Electron Trace gas chromatograph (GC) mass spectrometer (MS) equipped with a 30-m DB-5MS fused silica capillary column (0.32 mm ID, 0.25 μm film thickness). The carrier gas was He. The GC temperature program was as follows: injection at 60°C, 2 min. isothermal; heating from 60°C to 150°C at 15°C min^{-1}; heating from 150°C to 320°C at 4°C min^{-1}; 20 min. isothermal. Identification of compounds was based on comparison of mass spectra and GC retention times with published data. Compound-specific carbon isotope ratio analysis was performed with a Thermo Electron Trace GC coupled via a Thermo Electron GCC-II-interface to a Thermo Electron Delta^{plus} XP mass spectrometer. GC conditions were identical to those described above for GC/MS analysis. Carbon isotope ratios are given in δ notation ($\delta^{13}C$, ‰) relative to the PDB standard. Several CO$_2$ pulses of known $\delta^{13}C$ value at the beginning and end of each run were used for calibration. Instrument precision was checked using a standard *n*-alkane mix (*n*-C$_{15}$ to *n*-C$_{29}$ with known isotopic composition). Standard deviations of carbon isotopic measurements were <0.4‰. In the instrument time allotted for this study, we were unable to obtain replicate analyses of the biomarker isotope ratios. This work is planned as part of a future study.

[16] We calculated the isotopic fractionation (ε_p) associated with the photosynthetic fixation of carbon using the empirically derived equation (equation (1)) of *Freeman and Hayes* [1992], where δ_d is the isotopic composition of carbon in aqueous CO$_2$ and δ_p is the isotopic composition of photosynthate carbon:

$$\varepsilon_p = 10^3 \left[(\delta_d + 1000)/(\delta_p + 1000) - 1 \right] \qquad (1)$$

[17] It can be assumed for algae that intracellular CO$_2$(aq) reaches the photosynthetic site only by passive diffusion [*Raven and Johnston*, 1991], and therefore ε_p can be described as a simple equation (equation (2)) as proposed by *Bidigare et al.* [1997]:

$$\varepsilon_p = \varepsilon_f - b/C_e \qquad (2)$$

where ε_f is the carbon isotope fractionation due to the enzymes Rubisco and β-carboxylase, and its likely value ranges between 25 and 28‰ [*Goericke et al.*, 1994]. The range of values observed by *Goericke et al.* [1994] in various algae and cyanobacteria represents differences in carbon transport, fixation mechanism, cell size and/or growth rate. Because the physiological characteristics of ancient organisms are not constrained, the actual fractionation value for Cretaceous phytoplankton cannot be known. For all ε_p calculations, we assumed a value of 25‰.

Table 3. Sediment Composition and Component Isotopic Compositions[a]

Sample	Carbonate, wt %	TOC, wt %	$\delta^{15}N_{total}$	$\delta^{18}O_{carb}$	$\delta^{13}C_{carb}$	$\delta^{13}C_{org}$	$\delta^{13}C_{phytane}$
207-1257C-11R-1, 84–89	56.2	11.8	−2.0	−3.5	0.2	−26.7	−26.8
207-1257C-13R-2, 120–140	50.9	10.2	−1.8	−3.2	−0.6	−26.7	−29.7
207-1257C-14R-1, 76–82	35.5	13.7	−2.5	−2.9	−1.3	−28.1	−31.4
207-1258B-51R-2, 10–20	39.4	10.5	−2.4	−3.1	−0.2	−29.5	−29.1
207-1258B-54R-3, 10–30	47.8	9.3	−2.6	−3.0	−2.5	−29.7	−30.9
207-1258B-55R-3, 68–88	25.3	6.7	−1.1	−2.7	−0.6	−28.5	−30.1
207-1260B-34R-2, 10–17	56.6	11.0	−1.6	−4.1	0.1	−27.5	−27.4
207-1260B-37R-1, 10–16	38.9	11.9	−1.9	−3.1	0.5	−27.8	−30.0
207-1260B-38R-1, 84–86	47.2	21.6	−2.6	−3.0	0.2	−24.9	−30.3
207-1260B-39R-1, 115–122	64.7	9.2	−0.9	−3.5	0.3	−28.9	−31.9
207-1260B-41R-1, 114–120	60.1	10.5	−2.2	−3.7	0.6	−29.5	−29.8

[a]Nitrogen isotope values are expressed relative to atmospheric dinitrogen. Carbon and oxygen isotope values are relative to the PDB standard. TOC is total organic carbon.

(Assuming an ε_f value of 28‰ would decrease our final pCO_2 estimates by several hundred ppm.) Carbon dioxide partial pressure calculations were made using measurements of phytane (Table 3), a compound that represents diagenetic products of the phytyl side chain of chlorophyll derived from phytoplankton and/or cyanobacteria [*Brooks et al.*, 1969; *Peters and Moldowan*, 1993]. C_e is the external concentration of dissolved CO_2 ($C_e = [CO_2(aq)]$, and b represents the sum of physiological factors affecting the total carbon discrimination, primarily growth rate [*Rau et al.*, 1996; *Bidigare et al.*, 1997] and cell geometry [*Popp et al.*, 1998].

[18] In recent to subrecent sediments, b values derived for alkenones correlate with phosphate concentrations in surface waters [*Andersen et al.*, 1999], and phosphate concentrations in surface waters are positively correlated with surface sediment $\delta^{15}N$ values [*Andersen et al.*, 1999]. We applied these assumptions to our Cretaceous data in order to estimate b values from $\delta^{15}N$ (Table 3), which resulted in an average b value of 171.1 (±3.8 1σ). We note, however, that denitrification processes and nitrogen fixation in the water column and sedimentary diagenetic alteration can affect $\delta^{15}N$, making it a problematic proxy for nutrient utilization or carbon demand. For example, under suboxic conditions, ^{15}N enrichment due to denitrification might be a significant process [*Altabet et al.*, 1995]. However, as a first-order estimate here, we assume b = 170 for our ε_p calculations. Given uncertainties in the b value, it is important to note the linear effect of b on pCO_2: if b is decreased from 170 to 130, pCO_2 values we calculate below (section 3.3) decrease by 300 ppmv.

[19] The calculation of paleoceanic pCO_2 from sedimentary proxy parameters follows the procedure of *Jasper et al.* [1994]. The isotopic composition of carbon in $CO_2(aq)$ (δ_d) was calculated from the $\delta^{13}C$ record of planktonic foraminifera analyzed in each sample, assuming the temperature-dependent carbon isotope fractionation of $CO_2(aq)$ with respect to HCO_3^- ($\varepsilon_{b(a)}$) from *Mook et al.* [1974]:

$$\varepsilon_{b(a)} = (24.12 - 9866)/T(^\circ K) \tag{3}$$

[20] Calculations of pCO_2 were made using both paleotemperature estimates from foraminiferal $\delta^{18}O$ (with and without an adjustment for pH, section 3.1) and from Mg/Ca,

with various assumptions about the Mg/Ca ratio in Cretaceous oceans (section 3.2).

[21] The isotopic composition of the primary photosynthate (δ_p) requires knowledge of the isotopic fractionation between carbon in the phytoplankton cell and carbon in the bulk organic matter [*Hayes*, 1993; *Summons et al.*, 1994]. The isotope fractionation is defined as

$$\varepsilon_{biomarker} = [(\delta_{bulk} + 1000)/(\delta_{biomarker} + 1000) - 1]$$
$$* 1000 \sim \Delta\delta = \delta_{bulk} - \delta_{biomarker} \tag{4}$$

[22] The $\varepsilon_{Biomarker}$ is approximately equal to $\Delta\delta$. The primary photosynthate (δ_p) of phytane-producing phytoplankton organisms was estimated from results derived from laboratory experiments [*Bidigare et al.*, 1997; *Schouten et al.*, 1998]. Following *Popp et al.* [1999], we assume a constant value of 4 for $\varepsilon_{phytane}$, as found for phytol [*Schouten et al.*, 1998]. The isotopic fractionation accompanying photosynthetic carbon fixation of carbon (ε_p) was then calculated from the isotopic composition of the primary photosynthate (δ_p) and that of $CO_2(aq)$, δ_d (equation (1)). The ε_p values then can be translated into CO_2 concentrations given an estimated b value. Using equation (2) with a constant $\varepsilon_f = 25‰$ we obtained the $CO_2(aq)$ values. Finally, $CO_2(aq)$ was converted to pCO_2 values via Henry's Law using solubility coefficients calculated after *Weiss* [1974]. Within the uncertainty in our calculations, the pCO_2 calculated can be assumed to be equal to the atmospheric CO_2 concentration. In the modern ocean, surface water and atmospheric CO_2 have been observed to differ by only ±37 ppm [*Tans et al.*, 1990].

2.4. Bulk Carbonate and Organic Carbon Amounts and Isotopes

[23] To determine bulk carbonate and organic carbon amounts and carbon and nitrogen isotopic composition, splits of freeze-dried sediment samples were ground to a homogeneous powder with an agate mortar and pestle. Concentrations of calcium carbonate (Table 3) were measured using the procedure of *Müller and Gastner* [1971] in which a known weight of sediment is treated with 3N HCl to release a volume of CO_2 that is proportional to its carbonate content. The relative analytical precision for the analyses is ±2% [*Robinson et al.*, 2002]. The carbonate-free
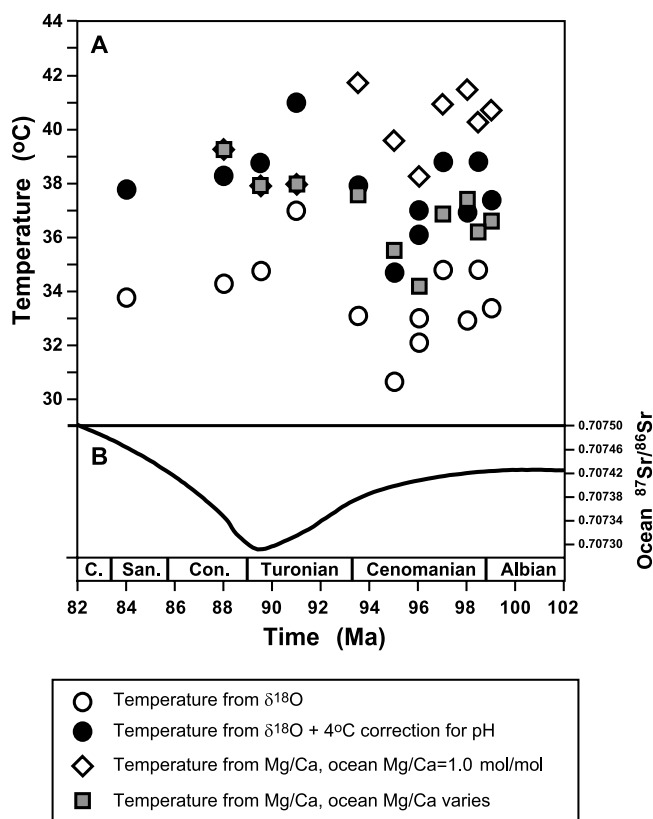
Figure 1. (a) Upper ocean temperature estimates through time from $\delta^{18}O$ and MgCa of planktonic foraminifera in the black shales. We consider the temperatures indicated by the solid circles and shaded squares to be more plausible (see text), but CO_2 calculations are performed using the full range of values shown here. The estimated uncertainty on the absolute ages of samples is less than 1 million years. (b) Ocean $^{87}Sr/^{86}Sr$ through time, from *McArthur et al.* [2001]. Values are relative to NIST 987 = 0.710248. The Turonian-Coniacian Sr isotope ratio minimum may coincide with a maximum in rate of seawater exchange through hydrothermal systems and a minimum in continental weathering rate, conditions which could also produce a minimum in seawater Mg/Ca ratio.

residue from this procedure was recovered by centrifugation, rinsed to remove chlorides, and dried for subsequent analyses. Total organic carbon amounts (TOC, Table 3) in the carbonate-free residue were determined with a Carlo Erba 1108 elemental analyzer in the Marine Geology and Geochemistry Laboratory at The University of Michigan. The absolute precision of the TOC analysis is ±0.05% [*Robinson et al.*, 2002]. TOC concentrations are expressed on a whole-sediment basis after adjusting for the carbonate content of each sample.

[24] Portions of the carbonate-free residue were analyzed for their nitrogen and carbon isotopic compositions (Table 3) using the elemental analyzer interfaced directly with a Micromass OPTIMA mass spectrometer in the Department of Earth Sciences, ETH Zürich. The $\delta^{15}N$ of each sample is expressed

relative to atmospheric dinitrogen (AIR), and the $\delta^{13}C$ is given relative to the PDB standard. Precision of both values is better than ±0.1‰ based on repeated analysis of standards.

[25] Carbon and oxygen isotope compositions of the carbonate contents of the black shale samples (Table 3) were analyzed after roasting the powdered samples at 375°C for 1 h under vacuum to remove volatile organic substances. The samples were then treated with phosphoric acid at 90°C on a VG Isogas autocarbonate preparation system in the ETH Stable Isotope Laboratory. The liberated CO_2 gas was analyzed with a VG PRISM isotope ratio mass spectrometer. Isotope ratios are expressed in standard δ notation in per mil (‰) relative to PDB. Analytical precision based on an internal reference standard (Carrara marble) is ±0.10‰ for $\delta^{18}O$ and ±0.05‰ for $\delta^{13}C$.

3. Environmental Estimates From Proxy Data

3.1. Tropical Paleotemperature Estimates From $\delta^{18}O$

[26] Paleotemperatures were first estimated using the average of the minimum and maximum seawater $\delta^{18}O$ values (−0.40‰ and −0.54‰ SMOW) calculated from the latitude-dependent adjustment [*Zachos et al.*, 1994] to an ice-free ocean (−1.25‰ SMOW), given the range of possible paleolatitudes calculated by *Suganuma and Ogg* [in press]. These isotopic paleotemperatures are indicated by the open circles in Figure 1a. The isotopic data suggest late Albian to early Cenomanian upper ocean temperatures of 33°−35°C, decreasing by ∼3°C in the Cenomanian, then increasing by ∼7°C to a peak in the middle to late Turonian. The lowest planktonic $\delta^{18}O$ values we obtained in the Cretaceous black shales were found in Turonian sample 207-1260B-34R-2, 10−17 cm. Here, *H. delrioensis* and *H. globulosa* average −4.82‰ and −4.73‰ PDB, respectively, based on five replicate analyses of each species [*Bice and Norris*, 2005]. Assuming local water $\delta^{18}O$ values between −0.40 and −0.54‰ SMOW, these data suggest upper ocean temperatures as high as 37°C at paleolatitude 11° N (±5°). Following the Turonian maximum, temperatures in our low-resolution data set appear to have cooled to 34°−35°C by the early Coniacian, at the same time that the plateau moved ∼1° latitude nearer the equator [*Suganuma and Ogg*, 2006]. Today, mean annual temperatures in the upper 40 m at Demerara Rise (∼9°N latitude) are between 27 and 27.5°C [*Antonov et al.*, 1998].

[27] Because of the relatively low carbonate ion activity in a high pCO_2 ocean, these isotopic paleotemperatures may have a cool bias [*Spero et al.*, 1997]. On the basis of a model using a compilation of low-latitude shallow water carbonate $\delta^{18}O$ [*Veizer et al.*, 1999] and the pH effect on fractionation shown by *Zeebe* [1999], *Royer et al.* [2004] estimated that the cool bias for the mid-Cretaceous ocean would be between 3° and 5°C. With the assumption of a higher pCO_2/lower pH ocean in the Cretaceous, we therefore make a uniform +4°C adjustment to our isotopic paleotemperature calculations (solid circles in Figure 1a). It should be noted, however, that recent experimental investigations and theory of oxygen isotope fractionation within the carbonic acid system [*Beck et al.*, 2005; *Zeebe*, 2005] suggest that the pH effect on carbonate $\delta^{18}O$ is not as
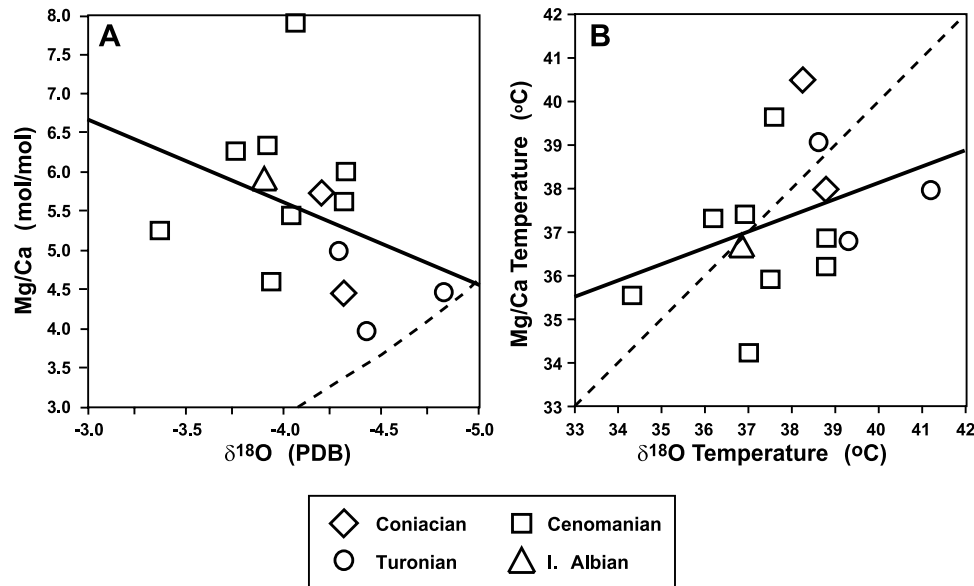
Figure 2. (a) Comparison of raw foraminiferal $\delta^{18}O$ and Mg/Ca data. The solid line indicates the best linear fit ($r^2 = 0.13$) to the raw data. The dashed line indicates a 1:1 correspondence of paleotemperature estimates from $\delta^{18}O$ and Mg/Ca, given some standard assumptions regarding Cretaceous ocean chemistry (see text). (b) Comparison of paleotemperature estimates from $\delta^{18}O$ with a +4°C adjustment for pH [*Royer et al.*, 2004] and Mg/Ca, assuming an ocean Mg/Ca value of 1.5 for the Albian and Cenomanian and 1.0 for the Turonian and Coniacian. The 1:1 temperature correspondence (dashed line) and best linear fit ($r^2 = 0.13$, solid line) are shown.

well understood as has previously been thought. Future revisions to the pH adjustment to Cretaceous paleotemperatures are therefore likely.

3.2. Tropical Paleotemperature Estimates From Mg/Ca

[28] Foraminiferal calcite $\delta^{18}O$ and Mg/Ca are both believed to record paleotemperatures, with local seawater $\delta^{18}O$ and ocean Mg/Ca representing additional unknowns in the paleotemperature equations. The nature of the two relations, based on observations from modern foraminifera, is such that more depleted carbonate $\delta^{18}O$ and higher carbonate Mg/Ca ratios indicate higher ocean temperatures. Figure 2a shows the relation between our raw Mg/Ca and $\delta^{18}O$ results of foraminifera from the same sediment samples. Instead of the expected positive slope to a best fit curve through the data as plotted, a negative relation (solid line) is observed, with, overall, low $\delta^{18}O$ corresponding to low Mg/Ca ratios. No systematic difference with species or with quality of foraminiferal preservation is seen in the $\delta^{18}O$:Mg/Ca relation (Table 1). A 1:1 temperature correlation (dashed line) is also shown in Figure 2a. This assumes no pH adjustment to temperatures calculated from $\delta^{18}O$. For Mg/Ca-based temperatures, the line assumes the *Elderfield and Ganssen* [2000] *G. sacculifer* relation, a Cretaceous ocean Mg/Ca ratio of 1.0 [*Stanley and Hardie*, 1998], a modern ocean Mg/Ca of 5.0, and that the *G. sacculifer* temperature:Mg/Ca relation scales linearly with ocean Mg/Ca. Given these assumptions, all the Mg/Ca paleotemperatures are warmer than those inferred from standard techniques of paleotemperature estimates from $\delta^{18}O$.

[29] An increase in the isotopic paleotemperatures of ~4°C to account for Cretaceous low pH ocean effects on oxygen isotope fractionation [*Royer et al.*, 2004] would improve the fit with paleotemperatures from Mg/Ca, but it cannot change the overall negative correlation between the two proxies. *Russell et al.* [2004] showed that for each 0.1 unit decrease in pH below a pH of 8.2, Mg/Ca increased by 7% (±5%) in cultured *Orbulina universa* to 16% (±6%) in *Globogerina bulloides*. This suggests that in oceans like the Cretaceous that might be expected to have higher pCO_2 and lower pH than the modern, uncorrected foraminiferal Mg/Ca will produce apparent warm temperatures. If the sensitivities observed by *Russell et al.* [2004] are representative of that of extinct Cretaceous planktonics, then the correction to Mg/Ca would be 2–22% for every 0.1 unit decrease in pH. Some pH correction (as yet unconstrained) to our values would bring the Mg/Ca paleotemperature estimates into better agreement with the isotopic paleotemperature estimates, as would the assumption of a Cretaceous ocean Mg/Ca ratio of 1.5 [*Dickson*, 2002]. However, as with the pH correction on $\delta^{18}O$, these uniform adjustments to estimates will not produce an overall correspondence of low $\delta^{18}O$ and high Mg/Ca.

[30] There is a great deal of time represented in the samples we are comparing, and it is possible that our assumption of a constant ocean Mg/Ca ratio over more than 10 million years is flawed. With that in mind, one possible interpretation of Figure 2a is that primarily Turonian and Coniacian analyses fall outside the expected low $\delta^{18}O$:high Mg/Ca relation. If the late Albian and Cenomanian ocean Mg/Ca was greater than that of the Turonian and Coniacian,

Mg/Ca-derived paleotemperatures from those older intervals would decrease relatively and improve the expected overall correspondence between high isotopic temperatures and high Mg/Ca-based temperatures.

[31] In Figure 2b we plot the Mg/Ca-based temperatures where an ocean value of 1.0 [*Stanley and Hardie*, 1998] is assumed for the Turonian and Coniacian, based on the expected correspondence of low Mg/Ca and low $^{87}Sr/^{86}Sr$ (further discussion below). For the Albian and Cenomanian, ocean Mg/Ca is assumed to equal 1.5 [*Dickson*, 2002]. The $\delta^{18}O$-based temperatures assume a uniform +4°C adjustment for low pH throughout the Albian-Coniacian interval. A 1:1 relation is indicated by the dashed line. An overall positive relation is now obtained between temperatures from the two proxies, and the variance around the best linear fit to the data (solid line in Figure 2b, $r^2 = 0.13$) is approximately ±2°C, or about the same magnitude as the estimated uncertainty in isotopic paleotemperature calibrations.

[32] We stress that variability in Cretaceous ocean Mg/Ca values is not the only possible interpretation of the unfortunately small data set shown in Figure 2, but there is a geological basis to hypothesize a difference between the Turonian-Coniacian ocean magnesium content and that of intervals above and below. Magnesium flux to the ocean is decreased through high rates of interaction of seawater with fresh basalt in mid-ocean ridge hydrothermal systems [*Hardie*, 1996] and during times of decreased continental weathering. The same relative changes in hydrothermal alteration and weathering will lead to a relative decrease in the seawater strontium isotope ratio ($^{87}Sr/^{86}Sr$). During periods of faster oceanic crust production at spreading centers, massive seafloor magma eruptions of large igneous provinces (LIPS), and lower continental weathering rates, both ocean Mg/Ca and $^{87}Sr/^{86}Sr$ should have decreased. It is therefore logical to consider the possibility that an ocean Mg/Ca minimum might have occurred along with the major negative inflection in the $^{87}Sr/^{86}Sr$ curve in the late Turonian–early Coniacian (Figure 1b) [*McArthur et al.*, 2001]. This local minimum is approximately coeval with extensive LIP and continental flood basalt eruptions that occurred in the late Turonian [92 Ma; *Phinney et al.*, 1999] and early Coniacian (88 Ma [*Courtillot et al.*, 1999]). Low ocean Mg/Ca and $^{87}Sr/^{86}Sr$ are also supported by a Late Cretaceous estimated terrigenous sediment flux rate ~35% lower than the modern, which would suggest decreased continental weathering, especially at times of relatively high sea level such as the late Turonian and the Coniacian [*Hancock and Kauffman*, 1979; *Kauffman and Caldwell*, 1993; *Miller et al.*, 2003, 2005]. A time period of very low continental erosion rates could also be expected to be an interval of relatively high atmospheric CO_2, since the removal of CO_2 through silicate weathering is the primary sink for CO_2 on timescales of millennia and greater.

[33] *MacConnell et al.* [2003] provide evidence of a possible secular change in ocean Mg/Ca within the Aptian-Albian (122–98 Ma) interval. Our data, and the occurrence of the ocean $^{87}Sr/^{86}Sr$ minimum in Turonian-Coniacian time (Figure 1b), suggest that a secular change is also plausible for the Cenomanian through Coniacian interval. However, more multiple proxy data are needed to confirm this change or to identify other possible explanations for discrepancies between foraminiferal $\delta^{18}O$ and Mg/Ca. Cretaceous ice sheet growth on Antarctica [*Stoll and Schrag*, 2000; *Miller et al.*, 2005] could be expected to increase mean seawater $\delta^{18}O$ but have no direct effect on ocean Mg/Ca molar ratios. This might cause a secular change in the relationship between foraminiferal $\delta^{18}O$ and Mg/Ca, which would best be detected in benthic taxa. Assuming an ice sheet mean isotopic composition between the modern Antarctic −50‰ [*Shackleton and Kennett*, 1975] and a more plausible warm climate value of −25‰ SMOW [*Bice*, 2004], an ice sheet volume change of 1 to 2 times that of the modern Antarctic ice would be needed to explain discrepancies of several degrees C between the two paleothermometers (Figure 2b). The estimated absolute age of only one of our samples (88 Ma, sample 207-1257C-13R-2) coincides with a sea level fall inferred by *Miller et al.* [2005] as plausibly due to growth of small ice sheets on Antarctica. There is therefore no strong evidence that the low-resolution data set described here contains evidence for Cretaceous ice sheet growth or decay.

[34] Regardless of which of our assumptions are accepted for calculating temperature from the two proxies, our data indicate that the Atlantic upper ocean waters at 9°–14° N (±5°) were at least 5°C warmer than modern conditions. A relative warming of 5°C was remarkable enough when paleogeographic reconstructions put Demerara Rise at 2°–5°N [*Norris et al.*, 2002; *Wilson et al.*, 2002], but ODP Leg 207 paleomagnetics now support a generally higher-latitude position for these sites in the mid-Cretaceous [*Suganuma and Ogg*, in press], forcing us to consider even lower pole to equator mid-Cretaceous temperature gradients than have been proposed in previous work [*Huber*, 1998; *Bice et al.*, 2003; *Jenkyns et al.*, 2004]. On the other hand, if Demerara Rise was located farther outside waters likely to have been cooled by equatorial upwelling, the Rise may provide a clearer record of tropical surface temperature changes than was previously thought [*Bice and Norris*, 2002].

[35] We emphasize that our calculations with foraminiferal Mg/Ca and manipulations of ocean Mg/Ca values are only experiments. We consider the application of the Mg/Ca paleotemperature proxy to Cretaceous and Paleogene climates to have significant outstanding uncertainties. There is, for example, the problem of not knowing the true Mg/Ca fractionation by extinct species. While we have assumed the *Elderfield and Ganssen* [2000] temperature equation for *G. sacculifer* Mg/Ca, *Dekens et al.* [2002] also derived a temperature correlation for core top *G. sacculifer*, one that includes a dissolution correction based on water depth in modern Atlantic specimens. Using their equation, and assuming a uniform paleowater depth of 2000 m for the three Demerara sites, our ratios yield temperature estimates that average ~7°C warmer than those obtained with the Elderfield and Ganssen equation. The uncertainty in our Mg/Ca-based paleotemperature reconstructions may therefore be quite large taking into account simply the range of calibrations available for one modern planktonic foraminifer.

[36] There is also the uncertainty in the true ocean Mg/Ca ratio, a potential pH control on magnesium incorporation [*Russell et al.*, 2004], and the possibility that temperature-
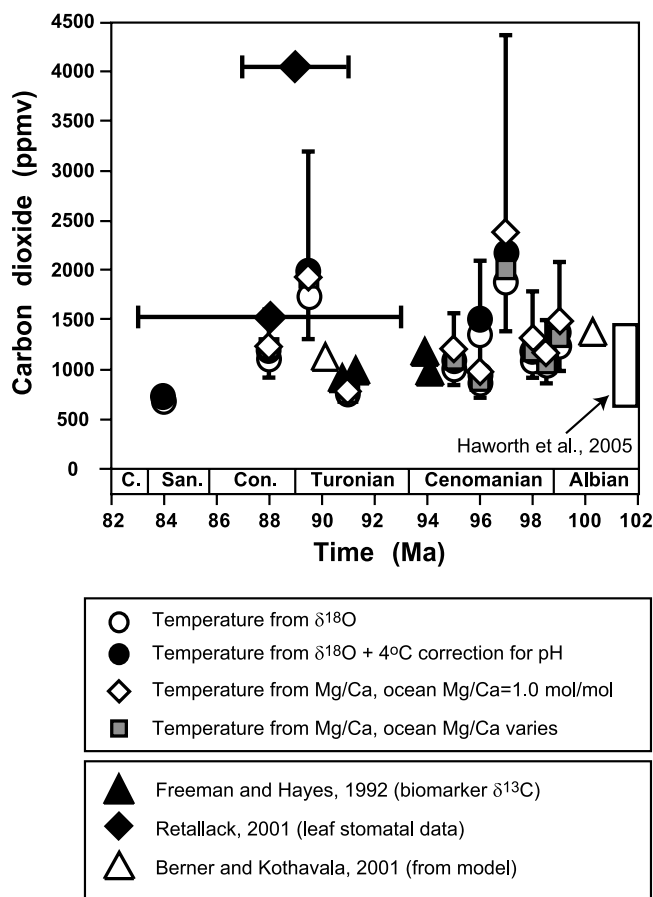
Figure 3. Atmospheric carbon dioxide estimates through time based on phytane $\delta^{13}C$ using an estimated b value (equation (2)) of 170 and four temperature estimates from foraminiferal $\delta^{18}O$ and Mg/Ca. The estimated uncertainty on the absolute ages of samples is less than 1 million years. The vertical error bars on Leg 207 data points are the sum of the uncertainty due to the analytical error in foraminiferal $\delta^{13}C$ ($\pm 0.03‰$) and phytane $\delta^{13}C$ ($\pm 1‰$) measurements. Published atmospheric CO_2 concentration estimates from other sources are shown for comparison.

dependent Mg fractionation in calcitic organisms varies nonlinearly with ocean Mg/Ca itself. Experiments by *Ries* [2004] have shown that the Mg fractionation coefficient for some modern groups varies with the ambient water Mg/Ca ratio. In echinoderms and decapods examined, the fractionation coefficient decreases with increasing seawater Mg/Ca, as it does in coralline algae [*Stanley et al.*, 2002], but the opposite relation is observed in grass shrimp. Given the estimated fivefold increase in Mg/Ca ratio between the Cretaceous and the modern ocean, it is possible that nonlinear ambient water-dependent corrections are needed for the proper application of Mg/Ca paleotemperature equations that are based on modern species [*Ries*, 2004].

[37] At the same time that we question the exact reconstruction of temperatures from Mg/Ca, it is important to bear in mind the possibility that the uncertainty in $\delta^{18}O$-based paleotemperature estimates is as large as that in any paleotemperatures we might infer from foraminiferal Mg/Ca. Problems include uncertainties in the true pH and $\delta^{18}O$ of ambient seawater on Demerara Rise through the broad time interval considered here, and the unknown temperature dependence of oxygen isotope fractionation in extinct foraminifera. The same uncertainties exist in any Cretaceous or Paleogene study in which these proxies are used, even when the foraminiferal calcite is believed to be preserved in good to excellent condition, as it is here. However, it is only by compiling, comparing and experimenting with such data that we can hope to gain confidence in or improve these proxy tools.

3.3. Estimates of Cretaceous Atmospheric Carbon Dioxide

[38] The next step in our multiproxy study requires paleotemperature as an input to the calculation of ancient CO_2. Given a variety of problems and uncertainties in the $\delta^{18}O$ and Mg/Ca proxies (discussed above), we look at the values of CO_2 predicted using the entire range of Cretaceous upper ocean temperature estimates. The temperatures assumed are those derived above: (1) the average from foraminiferal $\delta^{18}O$ calculated assuming seawater $\delta^{18}O$ values of $-0.40‰$ and $-0.54‰$ SMOW, (2) these same values increased by $4°C$ to account for possible pH effects on $\delta^{18}O$ [*Royer et al.*, 2004], (3) values from foraminiferal Mg/Ca assuming a constant Cretaceous ocean Mg/Ca ratio of 1.0, and (4) Mg/Ca-based paleotemperatures assuming an Albian/Cenomanian ocean Mg/Ca molar ratio of 1.5 and a Turonian/Coniacian ratio of 1.0. The resulting CO_2 estimates are shown in Figure 3. The low-resolution atmospheric CO_2 reconstruction shows variations between approximately 500 and 2500 ppmv, with possible local maxima in the Cenomanian (~ 97 Ma) and late Turonian (~ 89 Ma). Our lowest estimate occurs in the Santonian (~ 84 Ma), and a local minimum occurs in the Turonian (~ 91 Ma).

[39] The error bars shown in Figure 3 are conservative estimates resulting from the sum of uncertainties due to analytical error in foraminiferal $\delta^{13}C$ and biomarker $\delta^{13}C$ measurements. Additional error (not shown) exists due to uncertainty in the temperature estimate, which is poorly constrained but is often assumed to be $\pm 2°C$ for paleotemperature estimates from $\delta^{18}O$. Figure 4 illustrates the sensitivity of the CO_2 calculation to the three input variables derived from sample measurements (temperature proxies, foraminiferal $\delta^{13}C$ and biomarker $\delta^{13}C$). Calculated CO_2 is weakly nonlinear with respect to temperature and foraminiferal $\delta^{13}C$. Biomarker $\delta^{13}C$, on the other hand, exhibits a strong nonlinear control on CO_2. In calculating the solid curves in Figure 4, two variables were held constant at their average values and the third (the x axis variable) was allowed to vary over the range of measured in our samples. Of the three controlling variables, the uncertainty in the actual environmental temperature is the least well constrained source of error. For comparison, then, we also calculate the curves in Figures 4b and 4c assuming temperatures $5°C$ higher ($41°C$, upper dashed curves) and $5°C$ lower ($31°C$, lower dashed curves) than the approximate average from $\delta^{18}O$-based and Mg/Ca-based estimates.

[40] As is shown in Figure 4c, a temperature uncertainty of even ±5°C results in a calculated CO_2 error less than half that from the biomarker $\delta^{13}C$ analytical error (±1‰). In fact, if we assume a constant temperature equal to the approximate average of all values from each paleotemperature proxy technique, the resulting CO_2 estimates plot within the symbols used in Figure 3, differing by, at most, 150 ppmv from the values calculated using variable temperature estimates. The same is true if we assume a constant, average foraminiferal $\delta^{13}C$. The primary controlling variable on CO_2, as well as on CO_2 uncertainty, is the biomarker $\delta^{13}C$.
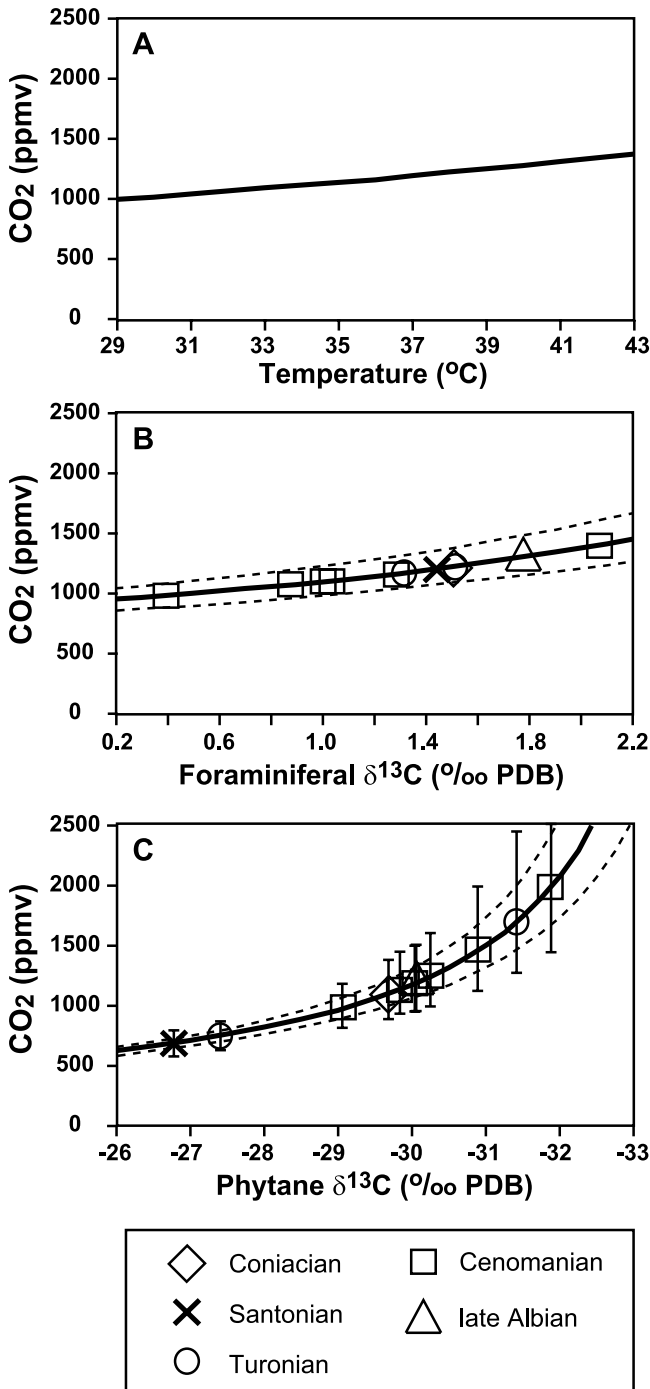
[41] Considering the analytical error on phytane $\delta^{13}C$, our late Albian through early Coniacian CO_2 estimates might allow for CO_2 over 4000 ppmv, or values might vary only between ~650 and 1400 ppmv. Ignoring the error, the second highest phytane $\delta^{13}C$ value (−27.4‰) occurs in Turonian sample 207-1260B-34R-2, 10−17 cm, and suggests a local CO_2 minimum of ~760−800 ppmv (±130 ppmv) (Figure 3), the second lowest estimate from our data. Surprisingly, though, this sample yielded the lowest planktonic $\delta^{18}O$ values we observed in the Cretaceous black shales (−4.82‰ in *H. delrioensis* and −4.73‰ in *H. globulosa*) and is generally coeval with Turonian evidence of extreme warmth from higher latitudes (see below). Foraminiferal $\delta^{18}O$ and Mg/Ca values from this sample suggest upper ocean temperatures of 37°−41°C (±2°C) (Figure 1a). If the best estimate of upper ocean temperature comes from the $\delta^{18}O$-derived estimates (with or without an adjustment for pH, section 3.1) and the Mg/Ca-derived estimates that assume a variable ocean Mg/Ca ratio (section 3.2), then the relative changes in tropical temperatures do not correlate well to relative changes in CO_2. If, on the other hand, ocean Mg/Ca was constant among the time intervals we have sampled, then there is an overall positive correlation between Mg/Ca temperatures and CO_2. On the basis of mid-Cretaceous climate model results [e.g., *Poulsen et al.*, 2001; *Otto-Bliesner et al.*, 2002; *Bice and Norris*, 2002] (see also new results below) as well as future climate model experiments [*Covey et al.*, 2003], there is no numerical model-based support for a negative correlation between tropical sea surface temperatures and atmospheric CO_2 concentration. There is therefore reason to suspect that the relative change in estimated pCO_2 from phytane $\delta^{13}C$ in sample 207-1260B-34R-2, 10−17 cm, is flawed. It is important to note that because temperature and CO_2 were estimated using data from the same samples, the apparent mismatch between high temperature and high CO_2 cannot be attributed to uncertainty in the age of the samples used for each proxy technique.

Figure 4. Single-variable sensitivity of the CO_2 calculation to (a) temperature, (b) foraminiferal $\delta^{13}C$, and (c) phytane $\delta^{13}C$. In calculations for Figures 4a–4c, only the x axis variable has been allowed to vary. In Figure 4a, temperature varies over the range of estimates shown in Figure 1, and in Figures 4b and 4c it is set equal to 36°C (solid line), 41°C (top dashed line), and 31°C (bottom dashed line). In Figure 4b, foraminiferal carbonate $\delta^{13}C$ varies over the range of values measured in our samples, and in Figures 4a and 4c it is set equal to its approximate mean $\delta^{13}C$ (1.3‰ PDB). In Figure 4c, phytane $\delta^{13}C$ varies over the range of values measured, and in Figures 4a and 4b it is set equal to its approximate mean value (−30‰ PDB). The positions of our Leg 207 data are indicated, by age, using open symbols in Figures 4b and 4c. In Figure 4b the uncertainty due to analytical error in foraminiferal $\delta^{13}C$ (±0.03‰) is less than ±10 ppmv, or well within the height of the symbols used. In Figure 4c the uncertainty due to analytical error in phytane $\delta^{13}C$ (±1‰) is indicated by the error bars on the Leg 207 data points.

[42] For comparison, some published atmospheric CO_2 estimates from other proxies in this time interval are shown in Figure 3. Our younger Cenomanian estimates and our lowest Turonian CO_2 estimate compare well to results by *Freeman and Hayes* [1992]. If the *Ginkgo pilifera* sample from Elistratova, Russia, measured by *Retallack* [2001] is late Turonian or Coniacian in age, then our CO_2 estimates are in good agreement. If, instead, this sample is mid-Turonian or Santonian in age, then Retallack's CO_2 estimate is at least 700 ppm higher than our estimates from Turonian sample 207-1260B-34R-2 and Coniacian sample 207-1257C-11R-1. Two other estimates published by Retallack that might be Turonian in age (one is shown in Figure 3) are ∼1000 to 3500 ppm higher than our highest Turonian estimate. It should be noted, however, that the small number of fossil fragments and the anomalous range of stomatal indices observed by *Retallack* [2001] in these samples casts some doubt on the reliability of those reconstructions [*Royer*, 2003].

[43] Estimates from the low temporal resolution (∼10 million years) carbon cycle model of *Berner and Kothavala* [2001] are in good agreement with a linear best fit to our CO_2 estimates through time, assuming any set of the temperature estimates. This result is in agreement with *Royer et al.* [2004], who argued that Phanerozoic atmospheric CO_2 reconstructions from various proxies, when averaged within 10 million year bins, compare reasonably well to CO_2 predictions from the carbon cycle model of *Berner and Kothavala* [2001], which is run with 10 million year time steps. However, temperature reconstructions for the Cenomanian through Turonian interval on Demerara Rise [*Norris et al.*, 2002; *Wilson et al.*, 2002] and Albian through Coniacian interval at high southern latitudes [*Huber et al.*, 1995; *Bice et al.*, 2003] suggest that a thermal maximum occurred in the middle to late Turonian. If changes in Cretaceous tropical upper ocean temperatures did correlate positively with changes in atmospheric CO_2 concentrations, then we expect a local CO_2 maximum in the middle to late Turonian, which would not be captured by a carbon cycle model based on averages over periods of 10 m.y.

[44] Other Cretaceous carbon dioxide estimates with age assignments that fall near or just beyond the temporal limits of the data shown in Figure 3 include Albian values of 1750 (±600) ppm [*Ekart et al.*, 1999], 600–1400 ppm [*Haworth et al.*, 2005], and 1000–2000 ppm [*Fletcher et al.*, 2005]. *Ekart et al.* [1999] obtained a Campanian CO_2 value of 1250 (±500) ppm, and *Yapp and Poths* [1996] calculated a Campanian value of 1400 ppm, with an error estimate of greater than 1000 ppm. In general, then, our new estimates are comparable to previously published values, but uncertainties in ages make a more definitive comparison with those values impossible.

4. Model-Data Comparisons

[45] GENESIS 2.0 climate model experiments were performed in order to determine the consistency, if any, between tropical temperatures and atmospheric CO_2 concentrations estimated here. By comparing the global model predictions to data from higher latitudes, we can also begin to say which model results are more or less plausible from a global climate perspective. The model and physical boundary conditions used here are the same as those used in mid-Cretaceous experiments described by *Bice and Norris* [2002] and *Bice et al.* [2003]. In the current experiments, however, the solar irradiance is set equal to 99.2% of the modern 1365 W m^{-2} [*Gough*, 1981]. The atmospheric carbon dioxide concentration was specified at levels from 1500 to 6500 ppm in single variable sensitivity tests. In most experiments, atmospheric methane was specified as 1.65 ppm, the approximate modern concentration. In several additional experiments, we investigated the effect of increased atmospheric methane by specifying a concentration of 50 ppm. In all experiments, the magnitude of the oceanic heat transport is equal to or less than that of the modern system [*Bice and Norris*, 2002]. Each experiment was run for at least 15 years after a steady state was reached in high-latitude surface temperature.

[46] The seasonal cycle results of GENESIS CO_2 experiments are shown in Figure 5. The results shown are the average of the final 10 years of monthly averages of steady state output. All CO_2 experiment curves shown differ by one standard deviation (0.2°–0.4°C) or more. It would not be meaningful to reproduce tropical temperatures alone, so to better evaluate the model, we add the constraint that model Arctic Ocean sea surface temperatures (paleolatitude ∼80°–85°N) should approximate estimates of 15°–25°C inferred for the mid- to latest Cretaceous by *Jenkyns et al.* [2004] and that model sea surface temperatures in the area of DSDP Site 511 (South Atlantic Falkland Plateau, paleolatitude ∼60°S) should be within those estimated using the oxygen isotope data of *Huber et al.* [1995] and *Bice et al.* [2003] (with no pH correction). Note that the age equivalence of any of our Leg 207 samples with those measured elsewhere cannot currently be constrained. These comparisons should therefore be considered preliminary, pending higher-resolution high-latitude data sets and better stratigraphic correlations between the tropical and higher-latitude sites.

[47] In general, the model underpredicts tropical Atlantic temperatures inferred from Leg 207 foraminiferal $\delta^{18}O$ and Mg/Ca when we specify approximate CO_2 concentrations estimated from the biomarker isotopes in the same samples. Coniacian and Santonian data suggest upper ocean temperatures 33°C and higher (Figure 1a) and biomarker $\delta^{13}C$ in these samples suggests CO_2 concentrations of 600–1500 ppm (Figure 3). However, with the modern CH$_4$ concentration, the model requires CO_2 concentrations to be at least 2500 ppm in order to simulate the estimated Coniacian and Santonian Demerara Rise temperatures (Figure 5a). With the modern CH$_4$ concentration, inferred Arctic Ocean temperatures of ∼16°–20°C are matched only when 4500 ppm CO_2 or more is specified to the model (Figure 5b). In contrast, with only 1500 ppm CO_2 (the maximum inferred from the biomarker data), the model predicts summer maximum temperatures that agree well with Coniacian/Santonian temperatures inferred for Falkland Plateau (Figure 5c); 2500 ppm CO_2 produces a good spring and summer seasonal match to the Falkland Plateau estimate.

[48] Our data suggest similar tropical temperatures (33°C or more) for the late Albian and earliest Cenomanian
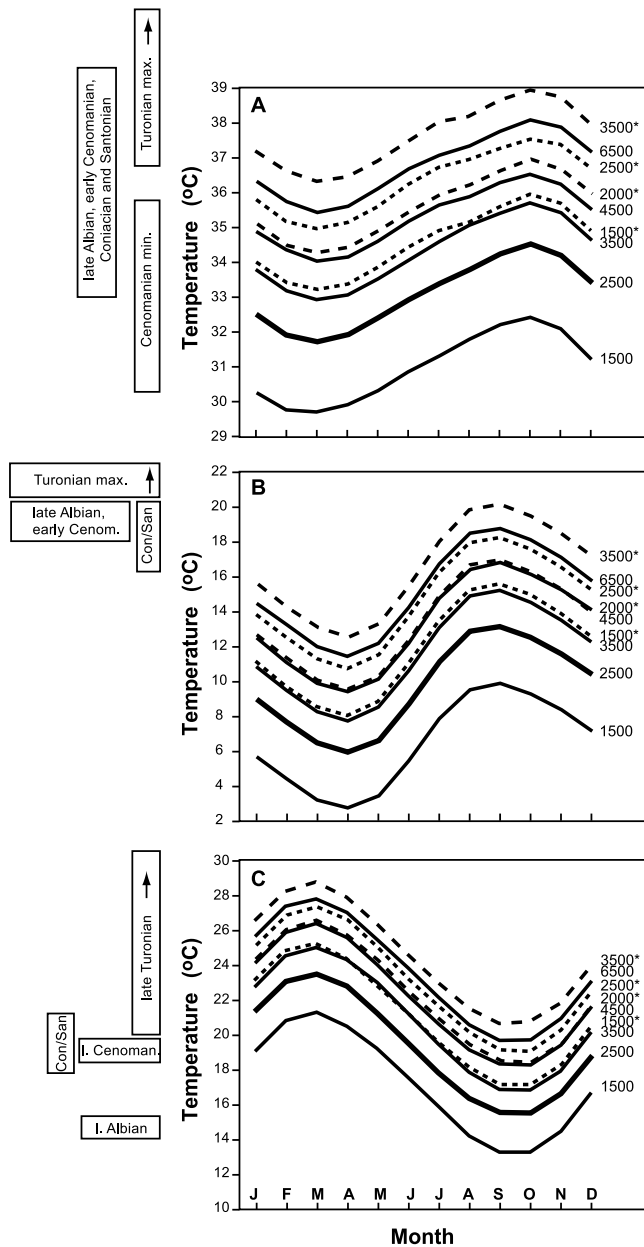
Figure 5. Seasonal cycle of ocean surface temperatures averaged over (a) Demerara Rise ($9°-14°$N, $65°-70°$W), (b) Arctic Ocean ($80-90°$N), and (c) Falkland Plateau ($55°-60°$S, $70°-75°$W). The specified CO_2 concentration is shown along the right margin: an asterisk indicates that CH_4 was specified at 50 ppm (dashed curves); otherwise, 1.65 ppm (solid curves) was used. Text boxes in the left margin indicate the ranges of paleotemperatures inferred for time intervals shown. Demerara Rise upper ocean temperature estimates are from this study. Falkland Plateau estimates are based on upper mixed layer dwelling planktonic δ^{18}O from DSDP Site 511 data (Cenomanian and late Turonian [*Bice et al.*, 2003] and l. Albian and Coniacian-Santonian [*Huber et al.*, 1995]). Arctic Ocean temperature estimates are from *Jenkyns et al.* [2004], based on Maastrichtian data and an assumed temperature gradient between southern England and the Arctic.

($\geq$98 Ma) (Figure 1a), and CO_2 is estimated as less than 2000 ppm based on biomarker δ^{13}C in these samples (Figure 3). However, again, the model requires CO_2 concentrations of at least 2500 ppm to attain a mean annual sea surface temperature of 33°C at Demerara Rise (Figure 5a). With only 1500 ppm CO_2, the model does a good job of matching the Falkland Plateau late Albian upper ocean temperature inferred from DSDP Site 511 planktonic δ^{18}O [*Huber et al.*, 1995] (Figure 5c), but the model's simultaneous underprediction of the late Albian tropical temperature indicates that the latitudinal temperature gradient in the model is too shallow. With 1500 ppm CO_2, the model underpredicts the inferred Arctic Ocean late Albian/earliest Cenomanian temperature by 8°C or more.

[49] For the late Turonian ($\sim$91 Ma), we noted above (section 3.3) the negative correlation between our maximum upper ocean temperature estimate and a very low CO_2 estimate (1000 ppm or less) from phytane δ^{13}C in the same sample. The climate model does not help us resolve this mismatch: In order to attain the minimum tropical temperatures suggested by the data from sample 207-1260B-34R-2, $10-17$ cm ($\sim$36°C, Table 2), the model requires $\sim$4500 ppm CO_2, if atmospheric CH_4 is specified at the modern concentration. To attain an isotopic paleotemperature that includes the pH correction or to match the Mg/Ca-based temperature estimate from this sample requires at least 5000 ppm CO_2 in the model. The model requires CO_2 concentrations of >4500 and >6500 ppm to approach the maximum temperatures inferred for the Turonian on Falkland Plateau and in the Arctic Ocean, respectively (Figures 5b and 5c). These results agree with previous model-data comparisons [*Bice and Norris*, 2002; *Bice et al.*, 2003] that showed that for this model, if only carbon dioxide is increased, concentrations of 4500 ppm or higher are needed in order to reproduce maximum mid-Cretaceous temperatures. Taking into consideration analytical uncertainty, the data might support maximum CO_2 concentrations of 3100 ppm (in the latest Turonian, 89.5 Ma) and 4400 ppm (in the Cenomanian, 97 Ma), but none of our phytane δ^{13}C data support CO_2 concentrations greater than 4500 ppm.

5. Discussion and Increased Methane Experiments

[50] There are several possible explanations for the model-data disagreement noted above. Sections 2 and 3 discuss the problems of inferring paleotemperature and paleo-CO_2 values from extinct species and ancient sediment organic matter. If our data interpretations are incorrect and the model sensitivity and model boundary conditions are reliable, the model-data comparison suggests that the inferred upper ocean temperatures are generally too high, the estimated atmospheric CO_2 concentrations are too low, or some combination of the two. In this "bad proxy/good model" case, the inferred upper ocean temperatures might be too high by $2°-8°$C in the tropics, by $6°-14°$C in the Arctic Ocean, and by $0°-10°$C over Falkland Plateau. Under these assumptions, the largest error occurs in the inferred Turonian temperatures and the smallest error is seen in Coniacian/Santonian temperatures. If, instead, all of the error is

in the proxy CO_2 estimates, then the inferred atmospheric CO_2 concentrations are too low by $1000-3000$ ppm in the Coniacian/Santonian and by at least 3500 ppm in the late Turonian.

[51] It is also possible that the model sensitivity to CO_2 is unrealistically low, such that not enough warming occurs when CO_2 is increased. With mid-Cretaceous boundary conditions and within the range of 500 to 5000 ppm CO_2, the GENESIS model exhibits an increase in global annual surface temperature of $2.4°-3.0°C$ in response to a doubling of CO_2 [Bice and Norris, 2002; this study]. If the model cloud response (parameterized in general circulation models) to water vapor increases is inappropriate given the magnitude of sea surface warming, then the model local radiative and/or latent heat transport responses might be unrealistic for higher levels of CO_2 forcing. We note, however, that if the nature of the model deficiency is an inadequate increase in total poleward heat transport with tropical warming, a "corrected" model would come closer to matching inferred high-latitude temperatures but would not match inferred tropical temperatures better without increased energy input to the tropics. The problem is then not simply insufficient poleward heat transport.

[52] Paleoclimate comparisons such as this are one of the few methods available for evaluating the quality of the response of a climate model (one that may also be used to predict future warming) to increased carbon dioxide concentrations. However, to conclude that the model sensitivity to CO_2 is too low based on such studies would require that we know our paleotemperature and paleo-CO_2 estimates to be accurate and that there be no significant error in the other model boundary conditions and model physics. Unfortunately, we cannot be sure that either condition is met.

[53] If the temperature and CO_2 proxy data (and our interpretations of them) are accurate, and the model sensitivity to CO_2 is accurate, then something else is missing in the model, something that will warm the surface about equally over these three disparate latitudes. The problem does not appear to be the lack of a fully coupled ocean-atmosphere in the model. Using the same atmospheric compositions, solar insolation, and very similar paleogeographies, we compared annual sea surface temperatures from GENESIS with those obtained by Otto-Bliesner et al. [2002] from Late Cretaceous (80 Ma) experiments with the Climate System Model (CSM) coupled ocean-atmosphere model. Mean annual sea surface temperatures predicted by GENESIS are within $2°C$ of those from CSM, and so the models agree within the uncertainty in the isotopic paleotemperature reconstructions. We must then consider other model boundary condition changes that would warm the surface about equally over the tropics and the two higher-latitude regions.

[54] Increasing solar luminosity to the modern value would warm the surface by $\sim0.5°C$, but modern-like luminosity is not supported by solar evolution models [Gough, 1981]. One more plausible candidate is increased atmospheric methane. In considering the Proterozoic atmosphere, Pavlov et al. [2003] suggest that when the oceans are oxygen and sulfate poor, there are fewer methanotrophs, a higher flux of methane to the atmosphere, a significantly

longer lifetime of atmospheric CH_4, and higher atmospheric CH_4 concentration. They show that atmospheric CH_4 concentration has a quadratic dependence on methane flux. For example, a tenfold increase in methane flux relative to the present would result in a sixtyfold increase in the atmospheric CH_4 concentration (to ~100 ppm). This represents the minimum flux increase suggested by Pavlov et al. [2003] for an oxygen-poor Proterozoic ocean with an order of magnitude lower sulfate concentration relative to the modern.

[55] Although sulfur isotope data are rare for mid-Cretaceous carbonates, studies by Gautier [1986] and Whittaker and Kyser [1990] suggest that dissolved sulfate was present at or near the seafloor in Cretaceous oceans. Evidence for the existence of a long-lived, largely anoxic water column is also not strong. Current data, then, do not support the absence of methanotrophic bacteria in the oceans during deposition of the Cretaceous black shales. However, given evidence that a shallow anoxic layer existed during times of black shale deposition, it is possible that greenhouse gases were generated higher in the water column than is the case today. Methane and dimethyl sulfide generation in the oxygen minimum zone (OMZ) would avoid extensive oxidation in the vast sub-OMZ ocean, perhaps allowing these gases to enter the atmosphere in significantly higher amounts. In fact, one possible interpretation of an overall up-section increase in bulk organic carbon through the Cenomanian-Turonian interval [Meyers et al., 2006] is that it reflects an overall decrease in methanotrophy. It appears reasonable, then, to consider the climate effects of an increased methane flux and atmospheric methane concentration for the intervals of Cretaceous black shale deposition. Another potential source of methane in the mid-Cretaceous is increased flux from low-lying wetlands [Ludvigson et al., 2002].

[56] Although possible abrupt changes in methane flux have been proposed within the Cretaceous [Beerling et al., 2002; Jahren, 2002; Weissert and Erba, 2004], background atmospheric methane concentrations are unconstrained. To obtain rough estimates of how much CH_4 (in addition to elevated CO_2 concentrations) is required to reproduce the inferred Cretaceous temperatures with the GENESIS model, we performed several experiments in which the atmospheric methane concentration was set to 50 ppm. This would imply an approximate 6.5-fold increase in methane flux, if the mid-Cretaceous atmospheric oxygen fraction was 0.1 to 1.0 relative to the present atmospheric level [Pavlov et al., 2003].

[57] The local seasonal sea surface temperature curves from increased methane experiments are shown by the dashed lines in Figure 5. Increasing the CH_4 concentration from the modern value (1.65 ppm) to 50 ppm has approximately the same sea surface warming effect as the increase in CO_2 from 1500 to 3500 ppm (Figure 5). Regardless of the CO_2 concentration, this increase in CH_4 warms Demerara Rise and the Falkland Plateau regions by $3.3°-3.8°C$ and warms the Arctic Ocean surface by $4.8°-5.5°C$. With 50 ppm CH_4, the model approximates the minimum inferred upper ocean temperatures from data when CO_2 concentrations are near those inferred using the biomarker proxy. The model matches or exceeds minimum inferred temperatures

for Demerara Rise and Falkland Plateau with 1500 ppm CO_2. For the Arctic Ocean, the model requires 2000 ppm CO_2 or more to approximate inferred minimum temperatures. In order to match the maximum upper ocean temperature estimates for the Cenomanian and Turonian, the model requires at least 3500 ppm CO_2 if the CH_4 concentration is 50 ppm.

[58] An additional potential effect of large increases in carbon dioxide [*Kirk-Davidoff et al.*, 2002] and, possibly, atmospheric methane [*Lelieveld et al.*, 1993] that is not included in our model is increased amounts of polar stratospheric clouds (PSCs), which would tend to preferentially warm the winter high latitudes. This problem was investigated for the Paleogene by *Peters and Sloan* [2000] using a version of GENESIS with noninteractive (prescribed) PSCs. Although this version of the model was available to us for Cretaceous experiments, *Kirk-Davidoff et al.* [2002] have raised questions regarding the adequacy of the stratospheric water vapor content in general circulation models when equator to pole temperature gradients are decreased to those typical of the Paleogene and Cretaceous. Their results using a two-dimensional model suggest that GENESIS and similar general circulation models may lack the proper stratospheric water vapor and cloud formation increases expected as a consequence of changes in vertical momentum flux and stratospheric overturning rates with decreased latitudinal and vertical temperature gradients. *Kirk-Davidoff et al.* [2002] suggest that the primary model deficiency in this case is the vertical resolution of the tropical tropopause. Questions also exist regarding the proper relation between PSC optical depth and stratospheric water vapor and aerosol concentration changes. The last decade has seen increased attention to these problems among the climate community, with significant advances being made using remote sensing. We have chosen to not include prescribed PSCs in our experiments pending significant improvements in the general circulation models in terms of both vertical resolution and PSC optical depth parameterizations. We note, however, that our model-data discrepancies (section 4) are consistent with the inadequate model water vapor responses to increased CO_2 proposed by *Kirk-Davidoff et al.* [2002]: Given CO_2 concentrations inferred from phytane $\delta^{13}C$, the model-data mismatch is greatest in the high-latitude Arctic. Of the three sites where we compare model results against proxy data, this is the region where increased stratospheric water vapor would have the greatest effect.

6. Concluding Statements

[59] More integrated numerical model and multiple proxy studies such as this should be encouraged. Our results highlight the need to revisit the uncertainties associated with the model response to increased greenhouse gases, the assumptions involved in the use of foraminiferal Mg/Ca and $\delta^{18}O$ as temperature proxies, and the reconstruction of atmospheric CO_2 from biomarker $\delta^{13}C$. Attention should be given to the fact that the correct correspondence, if any, between ambient water temperature and the Mg/Ca of test carbonate in extinct planktonic foraminifera is uncon-

strained. There is also uncertainty in the reconstruction of ancient ocean Mg/Ca, which is believed to have changed considerably on timescales of >10 million years, but may also have exhibited variations on the scale of a few million years. Our data, for example, suggest that the Mg/Ca ratio in the Turonian-Coniacian ocean may have been lower than in the Albian-Cenomanian ocean, perhaps coincident with an ocean $^{87}Sr/^{86}Sr$ minimum. Similar uncertainties remain with the oxygen stable isotope paleotemperature proxy: We are not sure of the actual isotope fractionation by extinct species and we must make assumptions about the isotopic composition and pH of ancient ambient seawater. If our data interpretations are incorrect and the general circulation model sensitivity and boundary conditions are reliable, the model-data comparison suggests that mid-Cretaceous inferred upper ocean temperatures are too high, estimated atmospheric CO_2 concentrations are too low, or some combination of the two.

[60] On the other hand, if the proxy reconstructions are largely correct, then a severe deficiency exists in our model and in similar general circulation models. In that case, the data-model comparison could be interpreted as evidence that the model sensitivity to CO_2 is unrealistically low, such that not enough warming occurs when CO_2 is increased. If correct, this conclusion would have serious implications for future climate studies in which the actual future warming from elevated atmospheric CO_2 concentrations may be much greater than that predicted by the models.

[61] Finally, if the temperature and CO_2 proxy data and our interpretations of them are accurate, and the model sensitivity to CO_2 is accurate, our results indicate that some additional climate forcing is required. A plausible explanation is increased atmospheric methane, sourced from either decreased methanotrophy in the Cretaceous ocean oxygen minimum zones or from terrestrial wetlands. There is currently no proxy record for paleomethane concentrations and so we have no direct way to access the plausibility of increased methane for the black shale intervals. For now, the best approach to this problem may be to better constrain likely methane fluxes and atmospheric O_2 in the Cretaceous. Efforts to better understand rates of marine methanogenesis and methanotrophy, as well as Cretaceous terrestrial methane fluxes should be encouraged. By better constraining these conditions during intervals characterized by abundant organic matter deposition in the open ocean, we can improve our understanding of the mechanisms that lead to ocean anoxic or dysoxia and the accompanying climate and biosphere feedbacks, and we will increase the value of the mid-Cretaceous record as a test case for climate model sensitivity to increased greenhouse gas concentrations.

References

Altabet, M. A., R. Francois, D. W. Murray, and W. L. Prell (1995), Climate related variations in denitrification in the Arabian Sea from sediment $^{15}N/^{14}N$ ratios, *Nature*, *373*, 506–509.

Andersen, N., P. J. Müller, G. Kirst, and R. R. Schneider (1999), Alkenone $\delta^{13}C$ as a proxy for past CO_2 in surface waters: Results from the Late Quaternary Angola Current, in *Use of Proxies in Paleoceanography: Examples From the South Atlantic*, edited by G. Fischer and G. Wefer, pp. 469–488, Springer, New York.

Antonov, J. I., S. Levitus, T. P. Boyer, M. E. Conkright, and T. O'Brien (1998), *World Ocean Atlas 1998*, vol. 1, *Atlantic Ocean Temperature Fields*, *NOAA Atlas NESDIS 27*, NOAA, Silver Spring, Md.

Beck, W. C., E. L. Grossman, and J. W. Morse (2005), Experimental studies of oxygen isotope fractionation in the carbonic acid system at 15°, 25°, and 40°C, *Geochim. Cosmochim. Acta*, *69*, 3493–3503.

Beerling, D. J., M. R. Lomas, and D. R. Groecke (2002), On the nature of methane gas-hydrate dissociation during the Toarcian and Aptian ocean anoxic events, *Am. J. Science*, *302*, 28–49.

Berner, R. A., and Z. Kothavala (2001), GEOCARB III: A revised model of atmospheric CO_2 over Phanerozoic time, *Am. J. Sci.*, *301*, 182–204.

Bice, K. L. (2004), The isotopic signal of glacioeustacy in the greenhouse world, paper presented at 8th International Conference on Paleoceanography, Cent. Natl. de la Rech. Sci., Biarritz, France. (Available at http://www.icp8.cnrs.fr/speaker_abstracts.pdf)

Bice, K. L., and R. D. Norris (2002), Possible atmospheric CO_2 extremes of the warm mid-Cretaceous (late Albian-Turonian), *Paleoceanography*, *17*(4), 1070, doi:10.1029/2002PA000778.

Bice, K. L., and R. D. Norris (2005), Data report: Stable isotope ratios of foraminifers from ODP Leg 207, Sites 1257, 1258, and 1260 and a cleaning procedure for foraminifers in organic-rich shales [online], in *Proc. Ocean Drill. Program Sci. Results*, *207*. (Available at http://www-odp.tamu.edu/publications/207_SR/104/104.htm)

Bice, K. L., C. R. Scotese, D. Seidov, and E. J. Barron (2000), Quantifying the role of geographic change in Cenozoic ocean heat transport using uncoupled atmosphere and ocean models, *Palaeogeogr. Palaeoclimatol. Palaeoecol.*, *161*, 295–310.

Bice, K. L., B. T. Huber, and R. D. Norris (2003), Extreme polar warmth during the Cretaceous greenhouse?: The paradox of the Late Turonian Record at DSDP Site 511, *Paleoceanography*, *18*(2), 1031, doi:10.1029/2002PA000848.

Bice, K. L., G. Layne, and K. Dahl (2005), Application of secondary ion mass spectrometry to the determination of Mg/Ca in rare, delicate, or altered planktonic foraminifera: Examples from the Holocene, Paleogene, and Cretaceous, *Geochem. Geophys. Geosyst.*, *6*, Q12P07, doi:10.1029/2005GC000974.

Bidigare, R. B., et al. (1997), Consistent fractionation of ^{13}C in nature and in the laboratory: Growth-rate effects in some haptophyte algae, *Global Biogeochem. Cycles*, *11*, 279–292. (Correction, *Global Biogeochem. Cycles*, *13*, 251.)

Boyle, E. A., and L. D. Keigwin (1985), Comparison of Atlantic and Pacific paleochemical records for the last 250,000 years: Changes in deep ocean circulation and chemical inventories, *Earth Planet. Sci. Lett.*, *76*, 135–150.

Boyle, E., and Y. Rosenthal (1996), Chemical hydrography of the South Atlantic during the Last Glacial Maximum: Cd vs. $\delta^{13}C$, in *The South Atlantic: Present and Past Circulation*, edited by G. Wefer et al., pp. 423–443, Springer, New York.

Brooks, J. D., K. W. Gould, and J. W. Smith (1969), Isoprenoid hydrocarbons in coal and petroleum, *Nature*, *222*, 257–259.

Courtillot, V., C. Jaupart, I. Manighetti, P. Tapponnier, and J. Besse (1999), On causal links between flood basalts and continental breakup, *Earth Planet. Sci. Lett.*, *166*, 177–195.

Covey, C., K. M. AchutaRao, U. Cubasch, P. Jones, S. J. Lambert, M. E. Mann, T. J. Phillips, and K. E. Taylor (2003), An overview of results from the Coupled Model Intercomparison Project, *Global Planet. Change*, *37*, 103–133.

Dekens, P. S., D. W. Lea, D. K. Pak, and H. J. Spero (2002), Core top calibration of Mg/Ca in tropical foraminifera: Refining paleotemperature estimation, *Geochem. Geophys. Geosyst.*, *3*(4), 1022, doi:10.1029/2001GC000200.

Dickson, J. A. D. (2002), Fossil echinoderms as monitor of the Mg/Ca ratio of Phanerozoic oceans, *Science*, *298*, 1222–1224.

Ekart, D. D., T. E. Cerling, I. P. Montanez, and N. J. Tabor (1999), A 400 million year carbon isotope record of pedogenic carbonate: Implications for paleoatmospheric carbon dioxide, *Am. J. Sci.*, *299*, 805–827.

Elderfield, H., and G. Ganssen (2000), Past temperature and $\delta^{18}O$ of surface ocean waters inferred from foraminiferal Mg/Ca ratios, *Nature*, *405*, 442–445.

Erbacher, J., et al. (2004), *Proceedings of the Ocean Drilling Program, Initial Reports* [online], vol. 207, Tex. A&M Univ., College Station. (Available at http://www-odp.tamu.edu/publications/207_IR/207ir.htm)

Erez, J., and B. Luz (1983), Experimental paleotemperature equation for planktonic foraminifera, *Geochim. Cosmochim. Acta*, *47*, 1025–1031.

Fletcher, B. J., D. J. Beerling, S. J. Brentnall, and D. L. Royer (2005), Fossil bryophytes as recorders of ancient CO_2 levels: Experimental evidence and a Cretaceous case study, *Global Biogeochem. Cycles*, *19*, GB3012, doi:10.1029/2005GB002495.

Freeman, K. H., and J. M. Hayes (1992), Fractionation of carbon isotopes by phytoplankton and estimates of ancient CO_2 levels, *Global Biogeochem. Cycles*, *6*, 185–198.

Gautier, D. L. (1986), Cretaceous shales from the western interior of North America: Sulfur/carbon ratios and sulfur-isotope composition, *Geology*, *14*, 225–228.

Goericke, R., J. P. Montoya, and B. Fry (1994), Physiology of isotope fractionation in algae and cyanobacteria, in *Stable Isotopes in Ecology and Environmental Science*, edited by K. Lajtha and R. H. Michener, pp. 187–221, Blackwell Sci., Malden, Mass.

Gough, D. O. (1981), Solar interior structure and luminosity variations, *Sol. Phys.*, *74*, 21–34.

Hancock, J. M., and E. G. Kauffman (1979), The great transgressions of the Late Cretaceous, *J. Geol. Soc.*, *136*, 175–186.

Hardie, L. A. (1996), Secular variation in seawater chemistry: An explanation for the coupled secular variation in the mineralogies of marine limestones and potash evaporites over the past 600 m.y., *Geology*, *24*, 279–283.

Haworth, M., S. P. Hesselbo, J. C. McElwain, S. A. Robinson, and J. W. Brunt (2005), Mid-Cretaceous pCO_2 based on stomata of the extinct conifer *Pseudofrenelopsis* (*Cheirolepidiaceae*), *Geology*, *33*, 749–752.

Hayes, J. M. (1993), Factors controlling ^{13}C contents of sedimentary organic compounds: Principles and evidence, *Mar. Geol.*, *113*, 111–125.

Huber, B. T. (1998), Tropical paradise at the Cretaceous poles?, *Science*, *282*, 2199–2200.

Huber, B. T., D. A. Hodell, and C. P. Hamilton (1995), Middle-Late Cretaceous climate of the southern high latitudes: Stable isotopic evidence for minimal equator-to-pole thermal gradients, *Geol. Soc. Am. Bull.*, *107*, 1164–1191.

Hut, G. (1987), Consultants group meeting on stable isotope reference samples for geochemical and hydrological investigations, report, 42 pp., Int. At. Energy Agency, Vienna.

Jahren, A. H. (2002), The biogeochemical consequences of the Mid-Cretaceous superplume, *J. Geodyn.*, *34*, 177–191.

Jasper, J. P., J. M. Hayes, A. C. Mix, and F. G. Prahl (1994), Photosynthetic fractionation of ^{13}C and concentrations of dissolved CO_2 in the central equatorial Pacific during the last 255,000 years, *Paleoceanography*, *9*, 781–798.

Jenkyns, H. C., A. Forster, S. Schouten, and J. S. Damste (2004), High temperatures in the Late Cretaceous Arctic Ocean, *Nature*, *432*, 888–892.

Kauffman, E. G., and W. G. E. Caldwell (1993), The western interior basin in space and time, in *Evolution of the Western Interior Basin*, edited by W. G. E. Caldwell and E. G. Kauffman, *Geol. Assoc. Can. Spec. Pap.*, *39*, 30 pp.

Kirk-Davidoff, D. B., D. P. Schrag, and J. G. Anderson (2002), On the feedback of stratospheric clouds on polar climate, *Geophys. Res. Lett.*, *29*(11), 1556, doi:10.1029/2002GL014659.

Lea, D. W., T. A. Mashiotta, and H. J. Spero (1999), Controls on magnesium and strontium uptake in planktonic foraminifera determined by live culturing, *Geochim. Cosmochim. Acta*, *63*, 2369–2379.

Lelieveld, J., P. J. Crutzen, and C. Bruhl (1993), Climate effects of atmospheric methane, *Chemosphere*, *26*, 739–768.

Ludvigson, G. A., L. A. Gonzalez, D. F. Ufnar, B. J. Witzke, and R. L. Brenner (2002), Methane fluxes from Mid-Cretaceous wetland soils: Insights gained from carbon and oxygen isotopic studies of sphaerosiderites in paleosols, *Geol. Soc. Am. Abstr. Programs*, *34*, 212.

MacConnell, A. B., R. M. Leckie, and J. Hall (2003), Submarine hydrothermal activity and secular changes in Mid-Cretaceous seawater chemistry, *Geol. Soc. Am. Abstr. Programs*, *35*, 204.

Martin, P. A., and D. W. Lea (2002), A simple evaluation of cleaning procedures on fossil benthic foraminiferal Mg/Ca, *Geochem. Geophys. Geosyst.*, *3*(10), 8401, doi:10.1029/2001GC000280.

McArthur, J. M., R. J. Howarth, and T. R. Bailey (2001), Strontium isotope stratigraphy; LOWESS version 3: Best fit to the marine Sr-isotope curve for 0–509 Ma and accompanying look-up table for deriving numerical age, *J. Geol.*, *109*, 155–170.

Meyers, P. A., S. M. Bernasconi, and A. Forster (2006), Origins and accumulation of organic matter in Albian to Santonian black shale sequences on the Demerara Rise, South American Margin, *Org. Geochem.*, in press.

Miller, K. G., P. J. Sugarman, J. V. Browning, M. A. Kominz, J. C. Hernandez, R. K. Olsson, J. D. Wright, M. D. Feigenson, and W. Van Sickel (2003), A chronology of Late Cretaceous sequences and sea-level history: Glacioeustasy during the Greenhouse World, *Geology*, *31*, 585–588.

Miller, K. G., M. A. Kominz, J. V. Browning, J. D. Wright, G. S. Mountain, M. E. Katz, P. J. Sugarman, B. S. Cramer, N. Christie-Blick, and S. F. Pekar (2005), The Phanerozoic record of global sea-level change, *Science*, *310*, 1293–1298.

Mook, W. G., J. C. Bommerson, and W. H. Stabermann (1974), Carbon isotope fractionation between dissolved bicarbonate and gaseous carbon dioxide, *Earth Planet. Sci. Letters*, *22*, 169–176.

Müller, G., and M. Gastner (1971), The "Karbonat-Bombe," a simple device for the determination of the carbonate content in sediments, soils and other materials, *Neues Jahrb. Mineral. Abh.*, *10*, 466–469.

Norris, R. D., K. L. Bice, E. A. Magno, and P. A. Wilson (2002), Jiggling the tropical thermostat during the Cretaceous hot house, *Geology*, *30*, 299–302.

Nürnberg, D., J. Bijma, and C. Hemleben (1996), Assessing the reliability of magnesium in foraminiferal calcite as a proxy for water mass temperatures, *Geochim. Cosmochim. Acta*, *60*, 803–814.

Otto-Bliesner, B. L., E. C. Brady, and C. Shields (2002), Late Cretaceous ocean: Coupled simulations with the National Center for Atmospheric Research Climate System Model, *J. Geophys. Res.*, *107*(D2), 4019, doi:10.1029/2001JD000821.

Pavlov, A. A., M. T. Hurtgen, J. F. Kasting, and M. A. Arthur (2003), Methane-rich Proterozoic atmosphere?, *Geology*, *31*, 87–90.

Peters, K. E., and J. M. Moldowan (1993), *The Biomarker Guide: Interpreting Molecular Fossils in Petroleum and Ancient Sediments*, 363 pp., Prentice-Hall, Upper Saddle River, N. J.

Peters, R. B., and L. C. Sloan (2000), High concentrations of greenhouse gases and polar stratospheric clouds: A possible solution to high-latitude faunal migration at the latest Paleocene thermal maximum, *Geology*, *28*, 979–982.

Phinney, E. J., P. Mann, M. F. Coffin, and T. H. Shipley (1999), Sequence stratigraphy, structure, and tectonic history of the southwestern Ontong Java Plateau adjacent to the North Solomon trench and Solomon Islands arc, *J. Geophys. Res.*, *104*, 20,449–20,466.

Popp, B. N., E. A. Laws, R. R. Bidigare, J. E. Dore, K. L. Hanson, and S. G. Wakeham (1998), Effect of phytoplankton cell geometry on carbon isotopic fractionation, *Geochim. Cosmochim. Acta*, *62*, 69–77.

Popp, B. N., et al. (1999), Controls on the carbon isotopic composition of Southern Ocean phytoplankton, *Global Biogeochem. Cycles*, *13*, 827–843.

Poulsen, C. J., E. J. Barron, M. A. Arthur, and W. H. Peterson (2001), Response of the mid-Cretaceous global oceanic circulation to tectonic and CO_2 forcings, *Paleoceanography*, *16*, 576–592.

Rau, G. H., U. Riebesell, and D. Wolf-Gladrow (1996), A model of photosynthetic ^{13}C fractionation by marine phytoplankton based on diffusive molecular CO_2 uptake, *Mar. Ecol. Prog. Ser.*, *133*, 275–285.

Raven, J. A., and A. M. Johnston (1991), Mechanisms of inorganic-carbon acquisition in marine phytoplankton and their implications for the use of other resources, *Limnol. Oceanogr.*, *36*, 1701–1714.

Retallack, G. J. (2001), A 300-million-year record of atmospheric carbon dioxide from fossil plant cuticles, *Nature*, *411*, 287–290.

Ries, J. B. (2004), Effect of ambient Mg/Ca ratio on Mg fractionation in calcareous marine invertebrates: A record of the oceanic Mg/Ca ratio over the Phanerozoic, *Geology*, *32*, 981–984, doi:10.1130/G20851.

Robinson, R. S., P. A. Meyers, and R. W. Murray (2002), Geochemical evidence for variations in delivery and deposition of sediment in Pleistocene light-dark color cycles under the Benguela Current Upwelling System, *Mar. Geol.*, *180*, 249–270.

Rosenthal, Y., E. A. Boyle, L. Labeyrie, and D. Oppo (1995), Glacial enrichments of authigenic Cd and U in subantarctic sediments: A climatic control on the elements' oceanic budget?, *Paleoceanography*, *10*, 395–413.

Rosenthal, Y., E. A. Boyle, and N. C. Slowey (1997), Temperature control on the incorporation of magnesium, strontium, fluorine, and cadmium into benthic foraminiferal shells from Little Bahama Bank: Prospects for thermocline paleoceanography, *Geochim. Cosmochim. Acta*, *61*, 3633–3643.

Royer, D. L. (2003), Estimating latest Cretaceous and Tertiary atmospheric CO_2 from stomatal indices, in *Causes and Consequences of Globally Warm Climates in the Early Paleogene*, edited by S. L. Wing et al., *Spec. Pap. Geol. Soc. Am.*, *369*, 79–93.

Royer, D. L., R. A. Berner, and D. J. Beerling (2001), Phanerozoic atmospheric CO_2 change: Evaluating geochemical and paleobiological approaches, *Earth Sci. Rev.*, *54*, 349–392.

Royer, D. L., R. A. Berner, I. P. Montanez, N. J. Tabor, and D. J. Beerling (2004), CO_2 as a primary driver of Phanerozoic climate, *GSA Today*, *14*, 4–10.

Russell, A. D., B. Hosnisch, H. J. Spero, and D. W. Lea (2004), Effects of seawater carbonate ion concentration and temperature on shell U, Mg, and Sr in cultured planktonic foraminifera, *Geochim. Cosmochim. Acta*, *68*, 4347–4361.

Schouten, S., W. C. M. Klein Breteler, P. Blokker, N. Schogt, W. I. C. Rijpstra, K. Grice, M. Baas, and J. S. Sinninghe Damste (1998), Biosynthetic effects on the stable carbon isotopic compositions of algal lipids: Implications for deciphering the carbon isotopic biomarker record, *Geochim. Cosmochim. Acta*, *62*, 1397–1406.

Shackleton, N. J., and J. P. Kennett (1975), Paleotemperature history of the Cenozoic and the initiation of Antarctic glaciation: Oxygen and carbon isotope analyses in DSDP Sites 277, 279, and 281, *Deep Sea Drill. Proj. Initial Rep.*, *29*, 743–755.

Spero, H. J., J. Bijma, D. W. Lea, and A. D. Russell (1997), Deconvolving glacial ocean carbonate chemistry from the planktonic foraminifera carbon isotope record, in *Reconstructing Ocean History: A Window Into the Future*, edited by F. Abrantes and A. C. Mix, pp. 329–342, Springer, New York.

Stanley, S. M., and L. A. Hardie (1998), Secular oscillations in the carbonate mineralogy of reef-building and sediment-producing organisms driven by tectonically forced shifts in seawater chemistry, *Palaeogeogr. Palaeoclimatol. Palaeoecol.*, *144*, 3–19.

Stanley, S. M., J. B. Ries, and L. A. Hardie (2002), Low-magnesium calcite produced by coralline algae in seawater of Late Cretaceous composition, *Proc. Natl. Acad. Sci. U. S. A.*, *99*, 15,323–15,326.

Stoll, H. M., and D. P. Schrag (2000), High-resolution stable isotope records from the Upper Cretaceous rocks of Italy and Spain: Glacial episodes in a greenhouse planet?, *Geol. Soc. Am. Bull.*, *112*, 308–319.

Suganuma, Y., and J. G. Ogg (2006), Campanian through Eocene magnetostratigraphy of Sites 1257–1261, ODP Leg 207, Demerara Rise (western equatorial Atlantic) [online], *Proc. Ocean Drill. Program Sci. Results*, *207*, in press.

Summons, R. E., L. L. Jahnke, and Z. Roksandic (1994), Carbon isotopic fractionation in lipids from methanotrophic bacteria: Relevance for interpretation of the geochemical record of biomarkers, *Geochim. Cosmochim. Acta*, *58*, 2853–2863.

Tans, P. P., I. Y. Fung, and T. Takahashi (1990), Observational constraints on the global atmospheric CO_2 budget, *Science*, *247*, 1431–1438.

Veizer, J., et al. (1999), $^{87}Sr/^{86}Sr$, $\delta^{13}C$ and $\delta^{18}O$ evolution of Phanerozoic seawater, *Chem. Geol.*, *161*, 59–88.

Wallmann, K. (2001), The geological water cycle and the evolution of marine $\delta^{18}O$ values, *Geochim. Cosmochim. Acta*, *65*, 2469–2485.

Weiss, R. F. (1974), Carbon dioxide in water and seawater: The solubility of an non-ideal gas, *Mar. Chem.*, *2*, 203–215.

Weissert, H., and E. Erba (2004), Volcanism, CO_2 and palaeoclimate: A Late Jurassic-Early Cretaceous carbon and oxygen isotope record, *J. Geol. Soc. London*, *161*, 695–702.

Whittaker, S. G., and T. K. Kyser (1990), Effects of sources and diagenesis on the isotopic and chemical composition of carbon and sulfur in Cretaceous shales, *Geochim. Cosmochim. Acta*, *54*, 2799–2810.

Wilson, P. A., R. D. Norris, and M. J. Cooper (2002), Testing the Cretaceous greenhouse hypothesis using glassy foraminiferal calcite from the core of the Turonian tropics on Demerara Rise, *Geology*, *30*, 607–610.

Yapp, C. J., and H. Poths (1996), Carbon isotopes in continental weathering environments and variations in ancient atmospheric CO_2 pressure, *Earth Planet. Sci. Lett.*, *137*, 71–82.

Zachos, J. C., L. D. Stott, and K. C. Lohmann (1994), Evolution of early Cenozoic marine temperatures, *Paleoceanography*, *9*, 353–387.

Zeebe, R. E. (1999), An explanation of the effect of seawater carbonate concentration on foraminiferal oxygen isotopes, *Geochim. Cosmochim. Acta*, *63*, 2001–2007.

Zeebe, R. E. (2005), Large effect of hydration on ^{18}O fractionation between H_2O and CO_3^{2-}: Implications for the pH-carbonate-$\delta^{18}O$ relationship and inferred climate changes, *Geophys. Res. Abstr.*, *7*, Abstract 03798.

K. L. Bice, Department of Geology and Geophysics, Woods Hole Oceanographic Institution, Woods Hole, MA 02543, USA. (kbice@whoi.edu)

D. Birgel and K.-U. Hinrichs, Research Center Ocean Margins, University of Bremen, PO Box 330 440, D-28334 Bremen, Germany.

K. A. Dahl, Scripps Institution of Oceanography, 9500 Gilman Drive, Department 0244, La Jolla, CA 92093, USA.

P. A. Meyers, Department of Geological Sciences, University of Michigan, 3514 CC Little Building, Ann Arbor, MI 48109, USA.

R. D. Norris, Scripps Institution of Oceanography, MS-0244, 308 Vaughan Hall, La Jolla, CA 92093, USA.